MODELING OF THE ROTARY-SCREW-DRIVEN DISPENSING PROCESS

A Thesis Submitted to the College of

Graduate Studies and Research

in Partial Fulfillment of the Requirements

for the Degree of Master of Science

in the Department of Mechanical Engineering

University of Saskatchewan

Saskatoon

By

Manouchehr Hashemi

PERMISSION TO USE

In presenting this thesis in partial fulfillment of the requirements for a postgraduate degree from the University of Saskatchewan, I agree that the libraries of this University may make it freely available for inspection. I further agree that permission for copying of this thesis in any manner, in whole or in part, for scholarly purposes may be granted by the professor who supervised my thesis work or, in his absence, by the head of the Department or the Dean of the College in which my thesis work was done. It is understood that any copying or publication or use of this thesis or parts thereof for financial gain shall not be allowed without my written permission. It is also understood that due recognition shall be given to me and to the University of Saskatchewan in any scholarly use which may be made of any material in my thesis.

Requests for permission to copy or to make other use of material in this thesis in whole or part should be addressed to:

Head of the Department of Mechanical Engineering

University of Saskatchewan

Saskatoon, Saskatchewan, S7N 5A9

ABSTRACT

Fluid dispensing is a process used to deliver fluid materials to targets such as substrates, boards, or work-pieces in a controlled manner. This process has been widely used in electronic packaging industry for such processes as integrated circuit encapsulation (ICE) and surface mount technology (SMT). The most important parameters needed to be controlled in this process are the flow rate of fluid dispensed and the profile of fluid formed on a target. The modeling and control of such a process involves different engineering disciplines including mechanical, control, software/hardware, and material science.

The present research is aimed to carry out a comprehensive study on the modeling of the rotary-screw dispensing system, in which a motor-driven screw is used to deliver fluid materials. At first, characterization of the flow behavior of fluids used in the electronic packaging industry is addressed. Under the assumption that the pressure applied to feed the fluid material has reached its steady state value, a steady state model is then developed to represent the flow rate of fluid dispensed in the rotary-screw dispensing process. On this basis, by taking into account the fluid compressibility and the fluid inertia, a dynamic model is developed to represent the dynamics of the flow rate, which is critical if the amount of fluid required to dispense is very small.

Experiments conducted on a typical commercial dispensing system of DS-500 (provided by Assembly Automation Limited, Hong Kong) were used to characterize the flow behavior of the fluid dispensed based on the model developed. The method of

identifying the flow behavior from dispensing experiments, rather than a rheometer, allowed the massive measurements needed in the use of rheometer to be eliminated.

To validate the steady state model, simulations were carried out in Matlab and the results were then compared with the experimental results obtained. It is shown that the simulation results are in qualifying agreement with the experimental results. Based on the dynamic model developed in this study, simulations were carried out to investigate the effects of operational parameters, such as temperature and fluid properties, on the flow rate of the fluid dispensed. Besides, the inconsistency in the fluid amount dispensed was also investigated by using the dynamical model. It has been shown that for dispensing small amounts of fluid, the dynamics of the flow rate dominate the process and that in this situation, the amount dispensed can be predicted by using the dynamic model developed and, in contrast, the use of the steady state model, which is commonly adopted in industry, can result in a large error in the model prediction.

Based on the dynamic model, a new approach is developed to integrate the model into the design of a fluid dispensing system. This approach could be used not only to evaluate existing dispensing systems, but also to design new dispensing systems.

ACKNOWLEDGMENTS

I am greatly thankful and indebted to my supervisor, Dr. Daniel Xiongbiao Chen, for providing me with an opportunity to work in his research lab and for his invaluable guidance, suggestions, and continuous encouragement. I wish to express my gratitude to the committee members Dr. Richard Burton and Dr. David Sumner, for their valuable suggestions during my master program.

I would like to extend my appreciation to my devoted wife Banafsheh Moazed for her continuous moral support and advice in the whole process.

I appreciate the support, love, patience, understanding and self-sacrifice of my parents, Abolhasan and Ashraf, who deserve a very special mention. I wish also to thank my sisters Rahele, Farzaneh and Farahnaz for their support during my master program.

TABLE OF CONTENTS

LIST OF TABLES

LIST OF FIGURES

NOMENCLATURE

A_n : needle cross-sectional area, m^2.

B : bulk modulus, Pa.

C_p : coefficient associated with the pure pressure-driven flow, m^3.

C_ω : coefficient associated with the pure drag flow, m^3.

D : feed tube diameter, m.

D_{sw} : screw tip diameter, m.

E_L : energy losses due to friction between the fluid and the needle wall, Pa.

$F_{d,p}$: shape factors for the drag and pressure flows, dimensionaless.

g : gravitational acceleration, m/s^2.

g_f : pressure gradient in the feed tube, Pa/m.

g_n : pressure gradient in the needle, Pa/m.

g_p : pressure gradient, Pa/m.

g_x : cross channel pressure gradients, Pa/m.

g_z : down channel pressure gradients, Pa/m.

H : flight height, m.

I : information content, bits.

K : consistency index, $Pa.s^n$.

L_f : feed tube length, m.

L_n : needle length, m.

L_s : syringe length, m.

L_z : channel length in z direction, m.

m : thixotropic index.

M : amount of fluid dispensed, kg.

M_c : magnitude of the control action, kg.

n : fluid index, dimensionless.

n_t : number of parallel threads, dimensionless.

P : pressure, Pa.

P_a : fluid pressure at the exit of the needle, Pa.

P_{aa} : ambient air pressure, Pa.

ΔP : pressure drop in the needle, Pa.

P_s : pressure in the fluid at the top of the syringe, Pa.

P_n : fluid pressure at the syringe bottom, Pa.

P_{mn} : pressure drop due to the effect of the entrance to the needle, Pa.

P_{mf} : pressure drop in feed tube due to the minor losses, Pa.

P_p : applied air pressure, Pa.

Q : flow rate, m^3/s.

Q_d : flow rate of the drag flow, m^3/s.

Q_n : flow rate in the needle, m^3/s.

Q_p : flow rate of pressure-driven flow, m^3/s.

Q_{pc} : pressure-driven flow due to the compressibility of the fluid inside the syringe, m^3/s.

Q_{pt} : total pressure-driven flow, m^3/s.

Q_{tube} : flow rate through the circular tube, m^3/s.

Q_s : steady state flow rate, m^3/s.

Q_u : steady-state flow rate under a unit pressure, m^3/Pa.

r : cone radius, m.

t : time, s.

T_d : dispensing time, s.

T : torque, N.m.

T_c : duration of the control action, s.

$u_{1,2}$: average velocities at the inlet and outlet of the needle, m/s.

u_t : average velocity of fluid in the feed tube, m/s.

u_n : average velocity of fluid in the needle, m/s.

V : velocity of the fluid flow in the needle, m/s.

V_b : velocity of the flat plate, m/s.

V_{bz} : speed of the barrel along down channel (z direction), m/s.

V_f : fluid volume inside the syringe, m^3.

V_x : velocity component in x direction, m/s.

V_z : velocity component in z direction, m/s.

W : channel width, m.

A_{cr} : area of common range, m^2.

DPs : design parameters, dimensionless.

FRs : functional requirements, dimensionless.

[A] : design matrix, dimensionless.

PDF : probability distribution density, dimensionless.

τ : shear stress, Pa.s.

τ_0 : yield stress, Pa.

τ_s : shear stress at the screw surface, Pa.

τ_w : shear stress at the needle wall, Pa.

τ_{yx} : shear stress in the plane of *yx*, Pa.

τ_{yz} : shear stress in the plane of *yz*, Pa.

μ : material viscosity, Pa.s.

ρ : fluid density, kg/m^3.

$\dot{\gamma}$: shear rate, s^{-1}.

ω : angular velocity, rad/s.

θ : angle of the cone, degree.

φ : helix angle of the screw, degree.

$\alpha_{1,2}$: kinetic energy correction factors at the inlet and outlet of the needle, dimensionless.

σ : fluid surface tension, Pa.

1. INTRODUCTION

1.1. Fluid Dispensing in the Electronics Packaging Industry

Fluid dispensing is a process that has been extensively used in industry for delivering various types of fluidic material to substrates, boards, or work pieces in a controlled manner. The materials used in this process range from watery liquids to thick pastes. Fluid dispensing is very important to industry including electronic packaging and food processing.

In the electronic packaging industry, for example, fluid dispensing is used in the process of die encapsulation in integrated circuit encapsulation (ICE). In this process, the wires bounded between the die and a substrate need to be encapsulated. The encapsulants used in the process have low ionic, low moisture absorbents, and low thermal expansion coefficient properties in order to protect the delicate areas from any environmental effect [Babiarz 1997, Babiarz and Huysmans 1997, Quinones et al. 2000]. Figure 1.1(a) shows a typical encapsulation procedure in ICE called “Dam and Fill”. A high viscosity encapsulant is dispensed on the substrate forming a dam around the die and wires, and another encapsulant with a low viscosity is dispensed inside the dam for the purpose of protection. Another application of fluid dispensing is in surface mount technology (SMT), which is shown in Figure 1.1(b). A small quantity of surface mount

adhesive needs to be dispensed between two conductive pads with a typical distance of 0.5-1.2 mm [Ness and Lewis 1997]. The adhesive material is used to secure the surface component to the board prior to wave soldering.

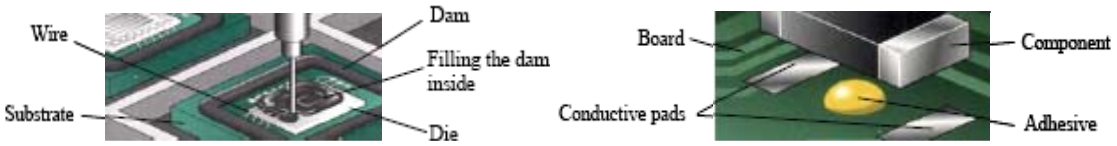

(a) (b)

Figure 1.1. Dispensing applications in the electronics packaging industry: (a) ICE, and (b) SMT.

In the typical applications of fluid dispensing, there are two very important performance indices: the flow rate of fluid dispensed and the profile of fluid formed on the target. The flow rate is critical and needs to be controlled in order to obtain the consistency and precision in the amount of fluid dispensed. It is desired that the flow rate is independent of the fluid properties such as density, viscosity, compressibility, etc. The profile of fluid formed is important from two aspects: 1) it should completely enclose the delicate area needing protection and 2) the profile contributes to the aesthetics of the final packaging.

1.2. Different kinds of Fluid Dispensing Systems

There are several types of dispensing systems reported in industry [Murch et al. 1997, Babiarz and Huysmans 1997, Ness and Lewis 1997, Krieger and Behler 1998, Chen et al.

1999]. Generally, the systems used in the electronic packaging industry can be classified, according to driving mechanisms, into three categories: time-pressure, rotary-screw, and positive-displacement, which are shown schematically in Figure 1.2.

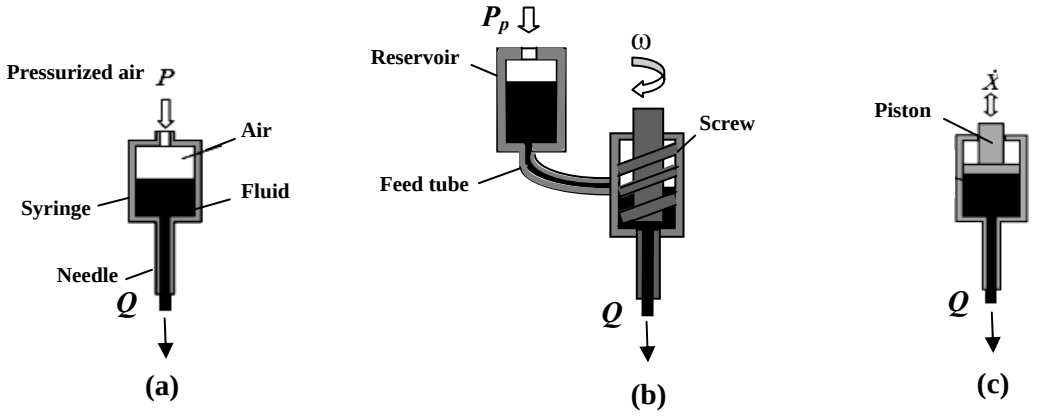

Figure 1.2. Schematic diagrams of the fluid dispensing systems: (a) time-pressure, (b) rotary-screw, and (c) positive-displacement

where Q is the flow rate, P is applied air pressure to the syringe, P_p is the air pressure applied to the reservoir, ω is the rotation speed of the screw, and $\dot{X}$ is the piston velocity. In the time-pressure dispensing system Figure 1.2a, pressurized air is used to force the fluid down the syringe and eventually out of the needle. In this type of system, the amount of fluid dispensed is defined by the magnitude and the duration of pressurized air. The advantages of this system include good adaptability, ease of maintenance, and the ability to dispense a very small amount of fluid. The main disadvantage of the system is that the compressibility of pressurized air and the viscosity of the fluid being dispensed can significantly affect the amount of fluid dispensed [Dixon et al. 1997, Chen et al. 2001 and 2002].

In the rotary-screw dispensing system Figure 1.2b, the rotation of a motor-driven screw causes the fluid to move down a syringe and then out of the needle. This approach is more stable than the time-pressure approach in terms of controlling of the fluid dispensed. However, due to high pressures produced in the fluid at the syringe bottom, causing an upward flow, this system is also influenced by the fluid viscosity [Li and Hsieh 1996, Babiarz 1997, Ness and Lewis 1997]. In spite of the above fact, the sensitivity of this system to the fluid viscosity is much less compared to the time-pressure system.

In the positive-displacement dispensing system Figure 1.2c, the movement of the piston is used to force the fluid in the syringe to move down and then out of the needle. The main advantage of this approach is that the amount of fluid dispensed is dependent only on the movement of the piston if a large amount of fluid needs to be dispensed. However, for small amounts of fluid, the amount of fluid dispensed is also influenced by the fluid compressibility and viscosity as well as the inertia of piston [Chen et al. 2003].

Theoretically, all of the aforementioned dispensing systems can deliver all fluids used in the electronic packaging industry. But, in practice, each of them may be excluded, depending on the type of fluid and/or the specific application [Bush 1997].

1.3. Rotary-Screw Dispensing System

1.3.1 An Overview of a Typical Rotary-Screw Dispensing System

The typical structure of a rotary-screw dispensing system is illustrated in Figure 1.3. In this system, pressurized air is applied to a reservoir, denoted (1); containing the fluid being dispensed, forcing the fluid down the material feed tube (2) and the feed shaft (3). In the syringe the fluid is forced by the rotation of the screw driven by a motor (6), then, fluid is moved down the threads of the screw (4) and eventually out of the needle (5). In comparison with the other two systems, i.e., time-pressure and positive-displacement dispensing systems, the rotary-screw dispensing system has the advantage of performing continuous dispensing without the need of refilling.

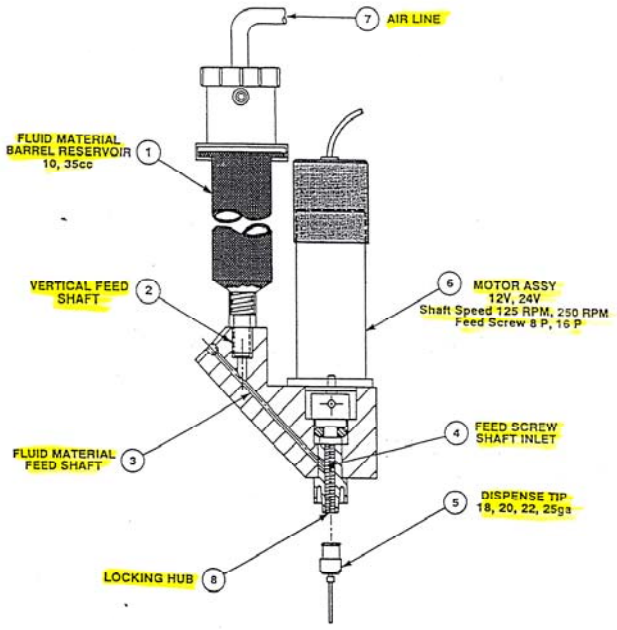

Figure 1.3. Typical structure of a rotary-screw dispensing system.

1.3.2. Modeling of the Flow Rate in a Rotary-Screw Dispensing System

In the rotary-screw dispensing system, there are some parameters that can significantly contribute to the flow rate or the amount of fluid dispensed. These parameters include the rotation speed of and geometry of the screw, the pressurized air applied to the system, and the flow behavior and compressibility of the fluid being dispensed.

If the leakage flow is ignored, the net flow in the screw channel is a combination of 1) the drag flow and 2) the pressure-driven flow, both of which act against each other. For the pressure-driven flow, the flow rate is dependent on the fluid viscosity. As a result, the rotary-screw system is not a true positive-displacement dispensing system, but a viscosity-dependent one. The following equation represents the flow rate in the rotary-screw dispensing system to dispense a Newtonian fluid assuming incompressible fluid, steady state fully developed and also one dimensional flow, which was developed by using the flat plate model [Rauwendaal 1986].

$$Q = n_t \frac{V_{bz} WH}{2} F_d + n_t \frac{WH^3}{12\mu}\left(-\frac{\partial P}{\partial Z}\right) F_p \tag{1.1}$$

where Q is the total flow rate, μ is the material viscosity, n_t is the number of parallel threads, V_{bz} is the speed of the barrel along down channel (z direction), W is the distance

between the threads, $\frac{\partial P}{\partial Z}$ is the internal pressure gradient along the screw channel, H is the distance between the thread root and the syringe wall, and $F_{d,p}$ are the shape factors for the drag and pressure flows, respectively. It should be mentioned that in the flat plate model, the syringe (barrel) is assumed to be unwrapped as a flat plate, which moves over the flat rectangular channel (screw channel). The first term on the right-hand side of Equation (1.1) is the flow rate due to the drag flow and is dependent on the screw geometry and the rotation speed. The second term is the pressure-driven flow and depends on the screw geometry and the fluid viscosity. The geometry of the screw in a rotary-screw dispensing system is shown in Figure 1.4.

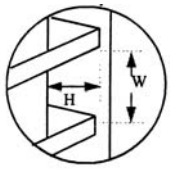

Figure 1.4. Geometry of the screw in a rotary-screw dispensing system.

In the previous model, the fluid is assumed as a Newtonian one. However, it should be noted that most fluids used in electronics packaging are usually non-Newtonian fluids. One characteristic that distinguishes a non-Newtonian fluid from a Newtonian one is the non-linear relationship between shear stress and shear rate. On this basis, non-Newtonian fluids can be classified in to three groups: 1) time-independent, 2) time-dependent and 3) Viscoelastic.

It is known that the viscosity of a fluid is defined as the ratio of the shear stress to the shear rate in the fluid. For a time-independent fluid, it is also called the "apparent viscosity". The most important characteristic of a time-independent fluid is the dependency of the viscosity on the shear rate and temperature. Various empirical models are developed in literature to describe this behavior. However, the model selected for the fluids used in electronic packaging should be easily integrated in the modeling of the fluid dispensing processes. One such model is the generalized power law model, given by Benezech and Maingonnat [1994], Tucker **[**1989] and Hong and Li [2003]:

$$\mu(\dot{\gamma}) = \mu_0 \qquad \tau < 2\tau_0^2$$

$$\mu(\dot{\gamma}) = K\dot{\gamma}^{n-1} + \frac{\tau_0}{\dot{\gamma}} \qquad \tau \geq 2\tau_0^2 \tag{1.2}$$

where μ is the viscosity, τ_0 is the yield stress, n is the fluid index, $\dot{\gamma}$ is the shear rate, and K is the consistency index. The above equation has the following features:

When $\tau_0 = 0$ and $n = 1$, it is the Newtonian model;

When $\tau_0 = 0$ and $n \neq 1$, it is the power law or Ostwald de Waele model;

When $\tau_0 \neq 0$ and $n = 1$, it is the Bingham model;

When $\tau_0 \neq 0$ and $n \neq 1$, it is the generalized power law or Herschel-Bulkley fluid model,

With three parameters of n, K, and τ_0.

For a given fluid, the values of n, τ_0 and K are determined experimentally. Specifically, n is usually identified as a constant, while τ_0 (with a unit of Pa) and K (with a unit of Pa·s^n) are functions of the temperature.

For time-dependent fluids, the viscosity is a function of both the magnitude and the time of applying shear, and sometimes it also depends on the time between the consequent applications of shear stress. Time-dependent fluids are classified into two groups: 1) thixotropic if the viscosity decreases with time, and 2) rheopectic if the viscosity increases with time. In electronic packaging, most of the time-dependent fluids show the thixotropic behavior. One promising model to describe the non-Newtonian behavior of time-dependent fluids is the time-dependent generalized power law equation, which was developed based on the generalized power law equation and is given by Rauwendaal et al. [1999]:

$$\tau = \tau_0 + K\dot{\gamma}^n t^{-m} \tag{1.3}$$

where t is the time, and m is the thixotropic index, giving the degree of time dependency.

During the past decades, many theories related to the rotary-screw driving system in the context of food processing have been developed. However, applying these theories to the screw design and simulations of industrial process has not been entirely successful [Rauwendaal 1989]. The first reason is that, due to the simplification of the existing theories, they are not accurate enough for the purpose of screw design and process

simulations. The second reason can be attributed to the fact that they are often misapplied to situations where their assumptions are not valid. The third reason is that the theories are mostly valid for only the steady state flow rate and cannot provide information about the dynamics of flow rate, which is particularly important when dispensing small amounts of fluid.

The "simplified flow theory" was first developed by Rowell and Finlayson [Rowell and Finlayson 1928] for screws with an infinite channel width. Although this theory is not based on the appropriate boundary conditions, its predictions of the volumetric flow rate are still reasonably accurate if applied to screws with a channel depth to radius ratio, H/R_b, of less than 0.05 [Li and Hsieh 1994]. A complete evaluation of the theory of boundary conditions [Rowell and Finalyson 1922] showed that the aforementioned solution for the screws with a finite channel width is not appropriate for the following reasons: 1) the screw flights were assumed to be stationary, which implies that the effect of the screw flights was not considered; and 2) the moving surface, which represents the outside cylinder, was assumed to have the velocity of the screw tip, $R_b\omega$. Many experimental results [Choo et al. 1980, McCarthy et al. 1992, Li and Hsieh 1996] have also shown that these assumptions are not appropriate.

Recently, to improve the accuracy of the flow rate, a special rotary-screw dispenser was designed, in which the three parts including outside body, screw flight, and screw core could be rotated separately as well as in pairs [Campbell et al. 1992]. It was found that the flow produced by the rotation of the screw was not compatible with the above mentioned existing theory, and that the screw flights were the major contributors to the

drag flow. Li and Hsieh [1996] developed a model in which the screw curvature was assumed to be small so that the barrel surface and the screw channel could be unwrapped and become flat plates. The prediction from the model was close to the experimental results published in literature. It is noteworthy to mention that this model as well as the previous ones assumes that the fluid material was Newtonian and are also valid for only the steady state flow, not the dynamic one.

Analysis of the non-Newtonian flow started in 1960. Generally, the developed equations could not be solved analytically and had to be solved by means of numerical techniques. The simplest non-Newtonian case that has been studied by many investigators was the one-dimensional isothermal flow of the power law fluid in a channel of infinite width. An exact analytical solution to even this simple problem has not been found to date [Rauwendaal 2004]. Also, studies have been carried out to investigate the two- or three-dimensional flows involving the assumptions of temperature-dependent viscosity and finite channel width [Rauwendaal et al. 1999]. However, these studies may not be applicable to the fluid manipulating processes that are encountered in industry. For example, the very simple analysis of "melt conveying" was first conducted for Newtonian fluids, and then was extended to the non-Newtonian behavior by using the "flat plate model", as presented in [Rauwendaal 2004]. It stated that, from the kinematics point of view, in the flat plate system the velocities and shear rates for both Newtonian and non-Newtonian fluids are different between the case where the barrel moves relative to a stationary screw and the case where the screw moves relative to the stationary barrel. If the root diameter is close to the barrel diameter, the difference between the two cases would be relatively small (about 10%). However, if the

root diameter is considerably smaller than the barrel diameter, the flat plate analysis with a moving screw results in a serious error. The reason is that the flat plate model can not account for the curvature of the channel. In a cylindrical system, there is no difference between velocities in the cases of rotating barrel and rotating screw [Rauwendaal 2004].

However, as mentioned before, all the models reviewed above are only valid for the steady state flow rate and cannot give any information about the dynamics of the flow rate, which is very important in electronic packaging.

1.4. Axiomatic Design of Fluid Dispensing Systems

Axiomatic design is one of the most powerful design methods which has been widely used in various engineering design processes, such as the design of software, manufacturing system, materials and materials-processing techniques, and products [Suh 2001]. In axiomatic design, the design process is defined as the mapping between the functional requirements (FRs) and the design parameters (DPs). The relationship between FRs and DPs are defined by design matrix [A]. There are two principles in axiomatic design which should be satisfied in each design process, i.e., the independence axiom and the information axiom. The independence axiom states that the independence of functional requirements must be maintained. To satisfy the independence axiom, the design matrix [A] must be either diagonal, in which the design is called uncoupled, or triangular, in which the design is called decoupled. Any other form of the design matrix does not meet the independence axiom and is called coupled design. For the task defined by a given set of FRs, it is likely that different designs can be result, all of which may be

acceptable in terms of the independence axiom. However, one of these designs is likely to be best. The information axiom states that, among the designs that are equally acceptable from the functional point of view, the design with the minimum information content is the best design.

As mentioned previously, there are three categories of fluid dispensing systems including time-pressure, rotary-screw and positive-displacement dispensing systems. There are various methods developed in the literature [Chen et al. 2002, Hong and Li 2003, Chen and Kai 2004] to model and control these systems to improve system performance. However, there is a lack of a method by which the designers and users could systematically evaluate and compare the three categories of dispensing systems in terms of the system performance. Obviously, the capability of doing such a thing would be of a great advantage for the designers when developing new dispensing systems, and for the users when choosing a specific dispensing system for their specific application. By applying the principles of axiomatic design, [Li et al. 2001] developed a conceptual approach to integrate the design and control of the fluid dispensing systems. In this approach, the time-pressure dispensing system was used, and a very simple model of the system was used to show the conceptual process, upon which the axiomatic design can be integrated to evaluate the system design and suggest an optimal system configuration with invariant properties to internal variations. Under minimal internal variation, the multivariable control that is intended to suppress external variations can be approximately constructed by a set of independent controllers to maintain a good performance in the dynamic environment. This conceptual approach was developed to integrate design and control methods for the time-pressure dispensing system. Apart

from the experimental verification of the approach, it gives no information about the rotary-screw and positive-displacement dispensing systems. As a result, it is impossible that the designers and users are able to systematically evaluate and compare the three categories of dispensing systems in terms of the system performance.

1.5. Research Objectives

The aim of this research is to carry out a comprehensive study on the modeling of the rotary-screw dispensing system. In particular, the objectives set to be achieved are described as follows:

1) Developing a steady state model to represent the flow rate of fluid dispensed under the assumption that the pressure applied to feed the fluid material has reached its steady state value. Based on this model, the influence of the flow behavior of the fluid being dispensed, the geometry of the screw and the applied air pressure on the flow rate can be specified.

2) Developing a dynamic model to represent the dynamics of the flow rate by taking into account the fluid compressibility and the fluid inertia. This model can be used to predict the fluid amount dispensed if the amount required to dispense is very small.

3) Evaluating the system performance of the rotary-screw dispensing system by means of the principles of axiomatic design, and then comparing to other different categories of dispensing systems.

1.6.Organization of the Thesis

This thesis consists of seven chapters. The following is a brief explanation of each chapter of the following.

Chapter 2 deals with the characterization of non-Newtonian flow behavior of the fluids used in the electronic packaging industry. Some existing models are examined and the method to determine the model parameters by using a rheometer is presented. Followed is the introduction to the method that is used in this study to determine the model parameter from a few dispensing experiments.

Chapter 3 presents the development of a steady state model for the flow rate of fluid dispensed under the assumption that the pressure applied to feed the fluid material has reached its steady state value. In particular, flow in screw channels and circular tubes is examined, and then the development of the model of flow rate of fluid dispensed is presented.

Chapter 4 presents the development of a model to represent the dynamics of the flow rate of fluid dispensed, by taking into account the fluid flow behavior, compressibility, and inertia.

Chapter 5 presents the experiments and simulations that were carried out in this study, in order to validate the models developed and investigate the performance of the rotary-screw dispensing system.

In Chapter 6, a new approach is presented, upon which the modeling and the design of the dispensing systems could be integrated. This approach is developed based on axiomatic design. Using this approach, a comparison is made to evaluate the three kinds of dispensing systems.

Chapter 7 presents the conclusions and the future work for this research.

2. CHARACTERIZATION OF THE FLOW BEHAVIOR OF FLUIDS USED IN THE ELECTRONIC PACKAGING INDUSTRY

Characterization of the fluids being dispensed is very important for modeling of fluid dispensing systems. Most of the fluids used in electronic packaging exhibit a non-Newtonian behavior. The characterization of such kind of behavior is discussed in this chapter.

2.1. Introduction to Fluid Behavior

As it was mentioned, most fluids used in electronic packaging are usually non-Newtonian with their most distinct characteristics of non-linear relationship between shear stress and shear rate. They were also classified in three groups: 1) purely viscous time-independent, 2) purely viscous time-dependent, and 3) viscoelastic [Skelland 1967, Barnes et al. 1989, Irvin and Capobianchi 1998, Chhabra and Richardson 1999].

In purely viscous time-independent fluids, the shear stress at a given point is only dependent on the instantaneous shear rate at that point. The ratio of shear stress to shear rate is also called the apparent viscosity or simply viscosity. The most important characteristic of time-independent fluids is the dependency of viscosity on the shear rate

and temperature. Figure 2.1 (a) shows the flow curves of several common time-independent fluids, in which $\tau_{\circ}$ is the yield stress.

In purely time-dependent fluids, the shear stress is a function of both the magnitude and the time of the applying shear rate, and sometimes it also depends on the time between the consequent applications of the shear stress. These fluids are classified into two classes: 1) thixotropic in which the viscosity decreases with the time, and 2) rheopectic in which the viscosity increases with the time. Figure 2.1 (b) illustrates the flow curves of these two classes.

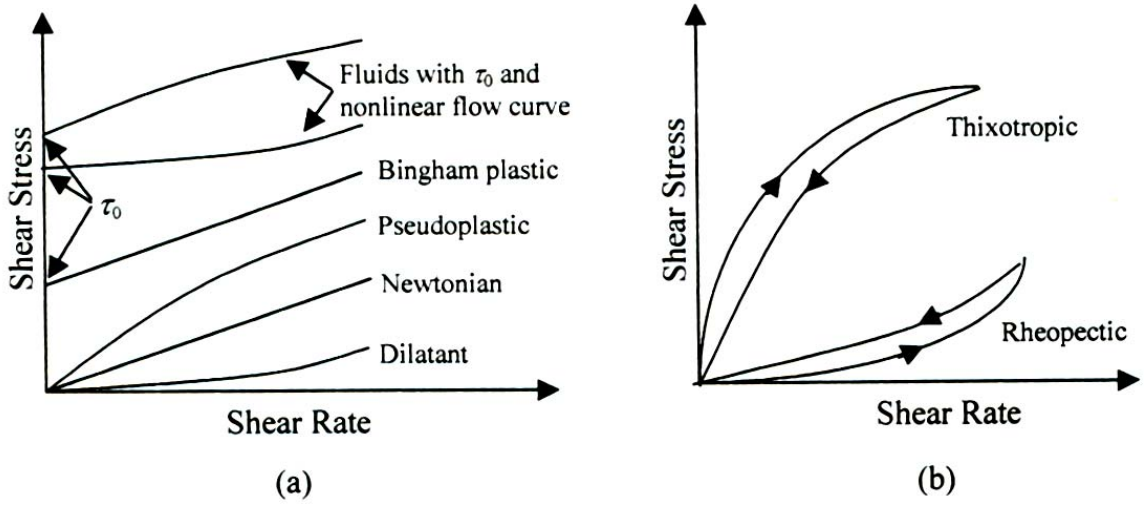

Figure 2.1. Flow curves of (a) time-independent fluids and (b) time-dependent fluids.

Viscoelastic fluids show partial elastic recovery once the force is removed. These materials show the properties of both fluids and elastic solids.

It is noteworthy to mention that the fluids used in electronic packaging are usually either time-independent or time-dependent materials. This research focuses on the time-independent flow behavior.

2.2. Characterization of the Time-Independent Non-Newtonian Behavior

Various empirical models have been developed for liquid food products in the literature [Holdsworth 1993, Benezech and Maingonnat 1994]. For the fluids used in electronic packaging, the model chosen for use should not only present the fluid non-Newtonian behavior but also be easily integrated in the modeling of the fluid dispensing processes. The power law equation is one of such models, which was used by Razban and Davis [1993 and 1995] to represent the behavior of Elastol M23 (supplied by Evode Ltd.). This equation is given by

$$\tau = K \dot{\gamma}^{n} \tag{2.1}$$

where τ and $\dot{\gamma}$ are the shear stress and shear rate in the fluid, respectively; K is the consistency index with a unit of $Pa \cdot s^n$, and n is the power law index (dimensionless). The value of n, ranging from 0 to 1, indicates the degree of non-Newtonian behavior; specifically, the greater departure of n from unity, the more pronounced the non-Newtonian behavior. If is n=1, the fluid is Newtonian and the consistency index K becomes the Newtonian viscosity.

Equation (2.1) can be used to describe the simple viscometric flow, in which the velocity components are in only one direction. For more complicated flow situations, more general power law expressions should be used. In the dispensing process by using the rotary-screw approach, the fluid flow in the screw channel could be considered as two-dimensional. In this situation, the power law equation has the following form [Rauwendaal 2004], if the fluid flows in the *x* and *z* directions

$$\tau = K\left[\left(\frac{dV_x}{dy}\right)^2 + \left(\frac{dV_z}{dy}\right)^2\right]^{\frac{n-1}{2}}\left(\frac{dV}{dy}\right) \tag{2.2}$$

where V_x and V_z are the velocity components in *x* and *z* directions, respectively. The direction of shear stress *(τ)* or velocity *(V)* is determined by the shear stress in the plane of *yz* (τ_{yz}) and the shear stress in the plane of *yx* (τ_{yx}). The magnitude of the total shear stress and the magnitude of the total velocity are, respectively, given by:

$$|\tau| = \sqrt{\tau^2{}_{yz} + \tau^2{}_{yx}} \tag{2.3}$$

$$|V| = \sqrt{V^2{}_{yz} + V^2{}_{yx}} \tag{2.4}$$

Another model that has commonly been used for the fluids used in electronic packaging is the generalized power law equation. This equation is given by:

$$\tau = \tau_0 + K\dot{\gamma}^n \tag{2.5}$$

where τ_0 denotes the yield stress. This equation was used by Han and Wang [1997a and b] to represent the non-Newtonian behavior of Hysol FP4510 (supplied by Dextor Corporation, USA), which is used for underfill encapsulation in electronics packaging.

2.3. Determination of the Model Parameters

To determine the parameters of a model for the flow behavior characterization, as given previously in Equations (2.1) and (2.5), there are two methods: 1) the use of a rheometer, and 2) the determination from the dispensing experiments.

2.3.1. Use of a Rheometer

There are various rheometerical approaches in industry to measure the non-Newtonian behavior of fluids experimentally. The basic features of these approaches can be found in some references [Skelland 1967, Barnes et al. 1989, Nguyn and Boger 1992, Holdsworth 1993]. The rheometer mainly consists of a cone, which rotates on a plate, as shown in Figure 2.2. The sample of a fluid is sheared within the gap between the cone and the plate. The angle of the cone is designed to be very small to ensure a constant shear rate throughout the shearing gap. This means that all fluid in the sample experiences the same shear history which is of great advantage when investigating time-dependent flow behavior. The measurement of the rheometer is based on the summation

of the torque over the conical surface as a function of the cone angular velocity, from which the flow curve of the shear stress vs. the shear rate is obtained. The shear stress is a function of torque, T, and the shear rate is a function of the angular velocity, ω. They are given by, respectively,

$$\tau = \frac{3T}{2\pi r^3} \qquad \text{and} \qquad \dot{\gamma} = \frac{\omega}{\sin\theta} \tag{2.6}$$

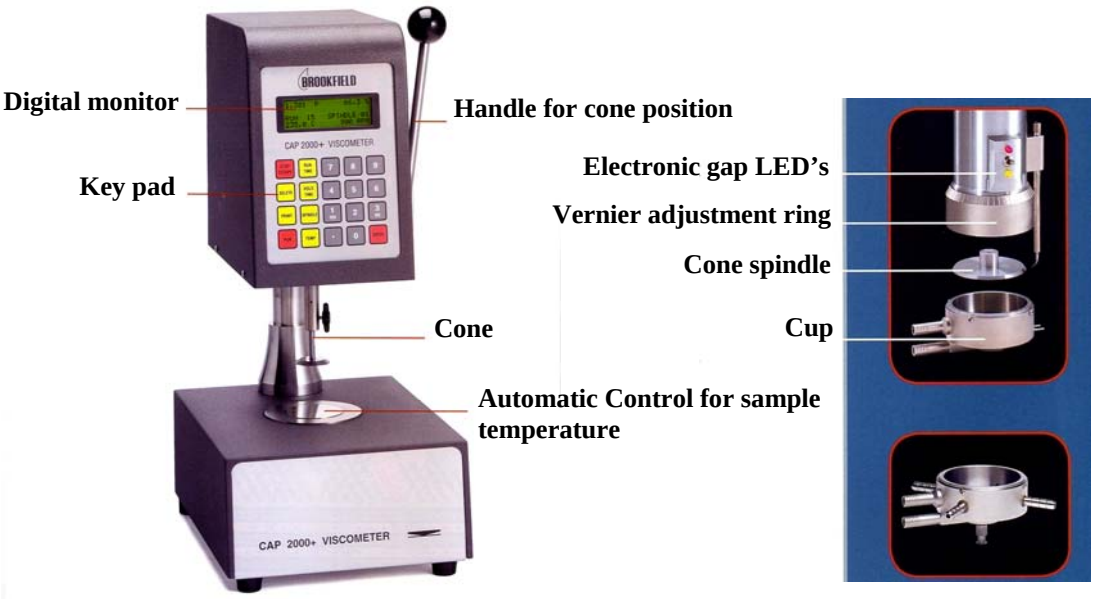

Figure 2.2. A rheometer provided by Brookfield Engineering Laboratories, INC.

Once the flow curve of the shear stress vs. the shear rate is obtained, the model parameters, e.g. K and n in Equation (2.1) or τ_0, K, and n in Equation (2.5), can be identified by using curve fitting. It should be noted that, in this method, the massive measurements in order to obtain the flow curve, are always required. Such a process has

proven to be time-consuming. Moreover, due to the sensitivity of flow behavior to temperature, the applications of the so-characterized fluid properties require that the temperature in the dispensing process be controlled as the same as the one in the rheometer. Otherwise, a little difference between them can result in a large error in the model prediction of the process performance by using the so-characterized flow behavior.

2.3.2. Determination from the Dispensing Experiments

In this study instead of using a rheometer, the fluid flow behavior is identified and characterized from a few dispensing experiments. The idea behind this method is that the fluid behavior can significantly affect the dispensing process and thereby, by monitoring the dispensing process, the fluid behavior can be identified. In this study, the flow rates in the dispensing process were measured, and based on the measured flow rates the flow behavior was then identified by means of the model developed for the dispensing process (which is presented in the following chapters). For the identification, the function of non-linear least-squares regression in Matlab was used to estimate the parameters associated with the flow behavior, which are K, and n, in Equation (2.1). This function estimates the parameters by starting with an initial guess and then altering the guess until the algorithm converges.

The experiments and results of determining the model parameters by using the above method are presented in Chapter 5. By experiments, this method has been shown not

only to be cost- and time-efficient but also promising for the characterization of fluids used in the dispensing process.

2.4. Summary

This chapter presents a brief introduction to non-Newtonian fluids. The distinct characteristic of these fluids is the non-linear relationship between shear stress and shear rate. The different types of these fluids commonly used in electronic dispensing process are discussed including time-dependent and time-independent materials. However, as the focus of this research is on the time-independent fluids, these types of fluids are discussed in detail. In the time-independent fluids, the viscosity is dependent on the shear rate and the temperature. The dependency of the viscosity on the shear rate and the temperature could be described by using the models of the power law equation and the generalized power law equation. To determine the model parameters, two different methods, i.e., 1) the use of a rheometer and 2) the determination from the dispensing experiments, are also briefly discussed in this chapter.

3. MODELING THE STEADY-STATE FLOW RATE IN THE ROTARY-SCREW DISPENSING SYSTEM

3.1. Introduction

The schematic of the rotary-screw dispensing system, considered in this study, is illustrated in Figure 3.1. Under the action of pressurized air provided by an air supply, the fluid inside the reservoir is fed to the screw channel through the feed tube. In the syringe, the fluid is then forced down the syringe by motor driven screw and eventually out of the needle. In this process, the flow rate of the fluid dispensed is an important measurement of the dispensing process performance. Due to the fluid compressibility, the pressure in the screw channel is gradually built until it reaches a steady state value. Therefore, the flow rate concerned is a dynamic one. In this chapter, it is assumed that the pressure in the screw channel has reached its steady state value; and a model is then developed to represent the steady state flow rate in the system. The dynamics of the flow rate is addressed in Chapter 4, by taking into account the fluid compressibility.

3.2. Modeling the Steady State Flow Rate of Fluid Dispensed

In this section, flow in screw channels and circular tubes are examined; and then the development of a model to represent the flow rate in the rotary-screw dispensing process is presented.

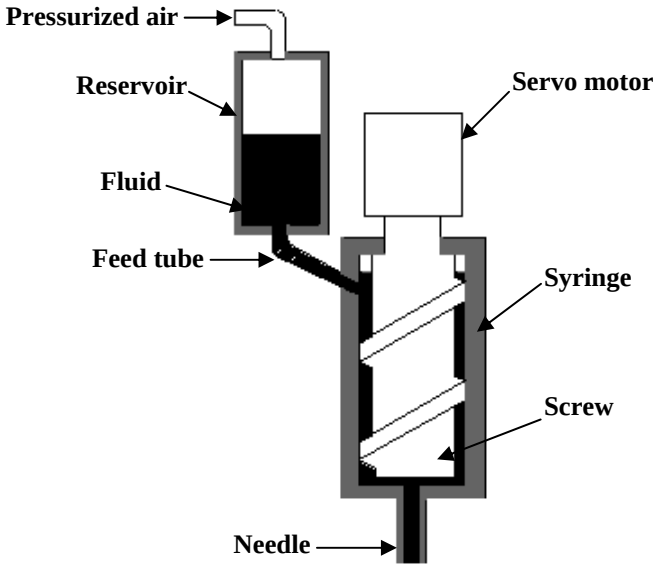

Figure 3.1. Schematic of a typical rotary-screw dispensing system.

3.2.1. Flow in Screw Channel

The geometry of the rotary-screw and the syringe is illustrated in Figure 3.2, in which W and H denote the channel width and flight height, respectively; L_s denotes the syringe length; L_n denotes the needle length; D_{sw} denotes the syringe internal diameter; and φ denotes the helix angle of the screw, P_s denotes the pressure in the fluid at the top

of the syringe, P_n denotes the fluid pressure at the syringe bottom; V_b denotes the velocity of the flat plate, and V_z and V_x denote the components of V_b along the direction of screw channel z and of channel width x, respectively. In this study, it is assumed that screw root and barrel surface can be approximated by flat plates, given that the screw depth is much smaller than the barrel internal diameter in a typical dispensing process. As was shown in previous study [Rauwendaal 2004], if the root diameter is considerably smaller than the barrel diameter, the flat plate analysis with a moving screw can result in a relatively large error; it is assumed in this study that the flat plate (barrel) moves over the flat rectangular channel (screw channel). Besides, it is also assumed that 1) the fluid is time-independent and in a steady laminar flow; 2) there is no slip between the fluid and the barrel wall; 3) the leakage flow through the gap between the flight and barrel is neglected; 4) the fluid flow is two dimensional, along the directions of down channel and cross channel. Based on the force balance, the fluid motion in the screw channel can be given by [Rauwendaal 2004]

$$\frac{\partial P}{\partial z} = g_z = \frac{\partial \tau_{yz}}{\partial y} \tag{3.1}$$

$$\frac{\partial P}{\partial x} = g_x = \frac{\partial \tau_{yx}}{\partial y} \tag{3.2}$$

where g_z and g_x are the down channel and cross channel pressure gradients, respectively, τ_{yz} and τ_{yx} are the shear stresses in the planes of yz and yx, respectively. Under these assumptions, the following boundary conditions are determined.

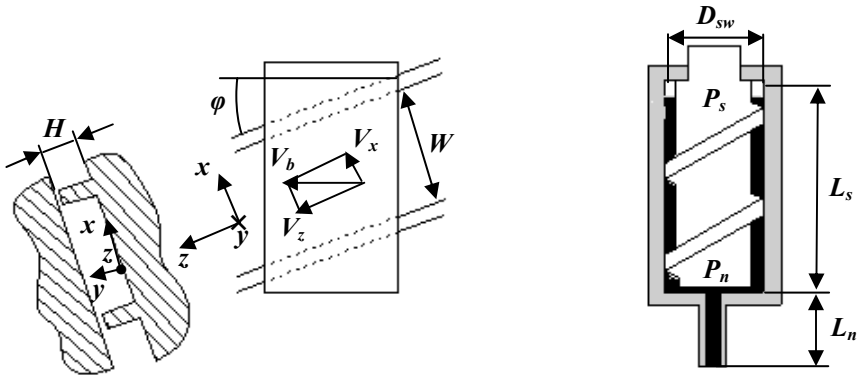

Figure 3.2. Geometry of the rotary-screw and the barrel.

$$V_z\Big|_{y=0} = 0$$

$$V_z\Big|_{y=H} = \frac{D_{sw}\omega\cos\varphi}{2} \tag{3.3}$$

$$V_x\Big|_{y=0} = 0$$

$$V_x\Big|_{y=H} = -\frac{D_{sw}\omega\sin\varphi}{2} \tag{3.4}$$

where ω is the screw rotational speed. If the leakage flow through the clearance between the flight and barrel is ignored, as assumed previously, then the net flow rate cross channel direction should be zero, i.e.,

$$\int_0^H V_x dy = 0 \tag{3.5}$$

Taking into account the Equations (3.1) and (3.2), the flow behavior Equation (2.2), the boundary conditions (3.3) and (3.4), and the zero flow rate in cross channel direction given in Equation (3.5), a numerical solution to the down channel velocity V_z can be obtained. Thus, by integrating it over the cross-sectional area of the screw channel, the flow rate in the down channel direction can be evaluated.

In order to find an analytical solution to the above problem, Rauwendaal [2004] presented a method which was developed for Newtonian flow and then it was modified by using correction factors for non-Newtonian flow. This method is summarized as follows:

In the screw channel shown in Figure 3.2, the fluid flow is a combination of the drag flow, which is the flow without a pressure gradient in down channel direction, and the pressure-driven flow, which is the flow without a relative motion between the screw and the barrel or the flow with zero screw speed. Thus, the net flow rate, Q, is given by

$$Q = Q_d - Q_p \tag{3.6}$$

where Q_d is the flow rate of the drag flow and Q_p is the flow rate of pressure-driven flow.

Under the assumption of infinite channel width, the fluid motion in the down channel direction z is governed by Equation (3.1) in which the fluid flow is assumed to be one dimensional and that the pressure is a function of only the down channel coordinate z. Therefore, Equation (3.1) can be integrated along y axis to give the shear stress profile in radial direction y as

$$\tau_{yz} = \tau_s + g_z y \tag{3.8}$$

where τ_s is the shear stress at the screw surface. If the fluid is considered Newtonian, then Equation (3.8) can be written as

$$\mu \frac{dV_z}{dy} = \tau_s + g_z y \tag{3.9}$$

where μ is the fluid viscosity, and V_z is the down channel velocity.

By integrating of Equation (3.9) along y axis, the down channel velocity as a function of normal distance y can be obtained. Then, using boundary conditions $V_z(0) = 0$ and $V_z(H) = V_{bz}$ yields

$$V_z(y) = \left[\frac{V_{bz}}{H} - \frac{g_z H}{2\mu}\right] y + \frac{g_z}{2\mu} y^2 \tag{3.10}$$

The flow rate in down channel direction is obtained by integrating the down channel velocity over the cross sectional area of the screw channel, which is given by

$$Q = \int_0^H W V_z dy = \frac{1}{2} W H V_z - \frac{W H^3 g_z}{12\mu} \tag{3.11}$$

If the pressure drop in down channel direction is considered linear, then g_z can be rewritten as

$$g_z = \frac{\Delta P}{L_z} \tag{3.12}$$

where ΔP is the pressure difference between syringe top P_s and syringe bottom P_n and L_z is the channel length in the z direction.

It should be noted that Equation (3.11) is derived for a Newtonian fluid. For no-Newtonian fluids, this relationship is unacceptably inaccurate if the fluid index n is less than 0.8 [Rauwendaal 2004]. In addition, the assumption of one-dimensional flow is accurate only for small helix angles, which are not in the range of the common helix angles used in the rotary-screw dispensing system. Thus, for accurate results, a two-

dimensional non-Newtonian analysis is recommended, in which numerical methods have to be employed.

In order to avoid complex calculations, an alternative method, is to use the Newtonian relationship Equation (3.11) with correction factors for non-Newtonian fluids. The correction factors were determined by Rauwendaal [2004] under the condition of minimizing the difference between one- and two-dimensional power law analyses to the helix angle in a range of 15° to 25°. Using the correction factors, one has

$$Q = (\frac{4+n}{10})WHV_{bz} - (\frac{1}{1+2n})\frac{WH^3}{4\mu}g_z \tag{3.13}$$

where n is the fluid flow index. In the right hand side of the above equation, the first term represents the drag flow rate and the second term represents the pressure-driven flow rate.

For the fluids with the flow behavior that is characterized by using the power law equation, the fluid viscosity, μ, is given by

$$\mu = K\left[\dot{\gamma}_{yz}\right]^{n-1} \tag{3.14}$$

where K is the consistency, and $\dot{\gamma}$ is the shear rate. Specifically in the rotary-screw dispensing process, $\dot{\gamma}$ is given by

$$\dot{\gamma}_{yz} = \frac{V_{bz}}{H} \tag{3.15}$$

where V_{bz} is the screw tip velocity and given by

$$V_{bz} = \frac{D_{sw}}{2}\cos\varphi \times \omega \tag{3.16}$$

Therefore, Equation (3.13) can be rewritten as

$$Q = \frac{(4+n)WHD_{sw}\cos\varphi}{20}\omega - \frac{WH^3}{4K(1+2n)}\left(\frac{D_{sw}\omega\cos\varphi}{2H}\right)^{1-n} g_z \tag{3.17}$$

From the above equation, it can bee seen that, the first term in the right-hand side, i.e., the flow rate due to the drag flow, is proportional to the screw rotational speed; and the second term, i.e., the flow rate due to the pressure-driven flow, is proportional to the pressure gradient. Thus, the flow rate in the down channel direction is determined by the screw rotation speed ω and the down channel pressure gradient g_z; meanwhile, it is also affected by the screw geometry D_{sw}, φ, W and H, and the flow behavior K and n.

3.2.2. Flow in Circular Tubes

Referring to the schematic of a dispensing system shown is Figure 3.3, it can be seen that both flows in the feed tube and the needle can be treated as the ones in circular tubes.

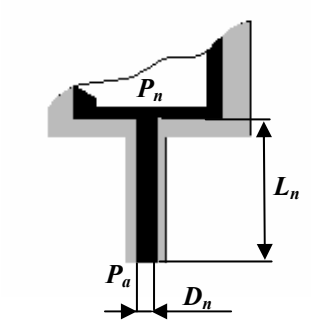

Figure 3.3. Schematic of pressure-driven flow in the needle.

where P_n denote the fluid pressure at the needle entrance, P_a denotes the fluid pressure at the needle exit, L_n and D_n denote the needle length and diameter respectively.

To represent the flow rate in the needle, it is assumed that 1) the fluid is incompressible and time-independent, 2) the fluid flow is in steady-state laminar flow, and 3) there is no slip between the fluid and the needle wall. Under above assumptions the total energy conservation at the needle inlet and outlet yields [Chen et al. 2002]

$$\frac{P_n}{\rho} + L_n g + \frac{u_1^2}{2\alpha_1} = \frac{P_a}{\rho} + \frac{u_2^2}{2\alpha_2} + \sum E_L \tag{3.18}$$

where ρ is the fluid density, g is the gravitational acceleration, $u_{1,2}$ and $\alpha_{1,2}$ are the average velocities and the kinetic energy correction factors at the inlet and outlet of the needle, respectively, and $\sum E_L$ is the sum of all energy losses due to friction between the fluid and the needle wall.

Taking into account the minor losses due to the effect of the needle entrance and exit, the pressure drop inside the needle ΔP can be derived from Equation (3.18) [Chen et al. 2002], which is given by

$$\Delta P = P_n - P_a + L_n \rho g - 1.12 \rho u_2^2 \tag{3.19}$$

If the flow behavior is characterized by a power law equation, the profile of velocity of the fluid flow in the needle V, as shown in Figure 3.4, can be obtained and given by Chen et al. [2002] as

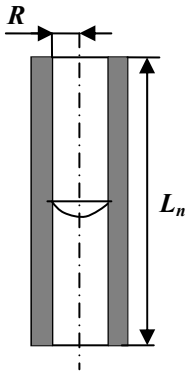

Figure 3.4. Profile of the fluid flow inside the needle.

$$V = \frac{2Ln}{K^{1/n}\Delta P(n+1)}\left[\left[\frac{R\Delta P}{2L_n} - \frac{r\Delta P}{2L_n}\right]^{(n+1)/n}\right] \quad \text{for} \quad 0 \le r \le R \tag{3.20}$$

To obtain the steady state flow rate through the circular tube, Equations (3.20) can be integrated over the cross section of the needle, i.e.,

$$Q = \int_0^R 2\pi r V dr \tag{3.21}$$

which yields

$$Q = \frac{n\pi R^3}{3n+1}\left(\frac{\tau_w}{K}\right)^{1/n} \tag{3.22}$$

where τ_w is the shear stress at the needle wall under the applied pressure, which can be derived based on minor losses due to the effect of the needle entrance and exit which is given by

$$\tau_w = \frac{D_n}{4L_n}(P_n - P_a + L_n\rho g - 1.12\rho u^2) \tag{3.23}$$

Substituting Equation (3.23) into Equation (3.22) can result in general Equation for the flow rate in the circular tubes including needle and feed tube [Chen and Hashemi 2005] as

$$Q_{tube} = \frac{\pi n D_n^{(3n+1)/n}}{2^{(3n+2)/n}(3n+1)K^{1/n}}(-g_p)^{1/n} \tag{3.24}$$

where Q_{tube} is the flow rate through the circular tube, D the tube diameter, and g_p the pressure gradient in the tube. It can be seen that flow rate is determined by the pressure gradient g_p, and is also affected by the tube diameter D and the flow behavior K and n.

3.2.3. Steady State Flow Rate of Fluid Dispensed

In order to derive an expression for the flow rate of fluid dispensed, the pressures of interest are shown in Figure 3.5, in which P_p is the applied air pressure, P_s the fluid pressure at the entrance to the screw channel, P_n the fluid pressure at the entrance to the needle, and P_a the fluid pressure at the exit of the needle, Q denotes the flow rate of fluid out of the needle, or the flow rate of fluid dispensed; the geometrical parameters are self-explanatory.

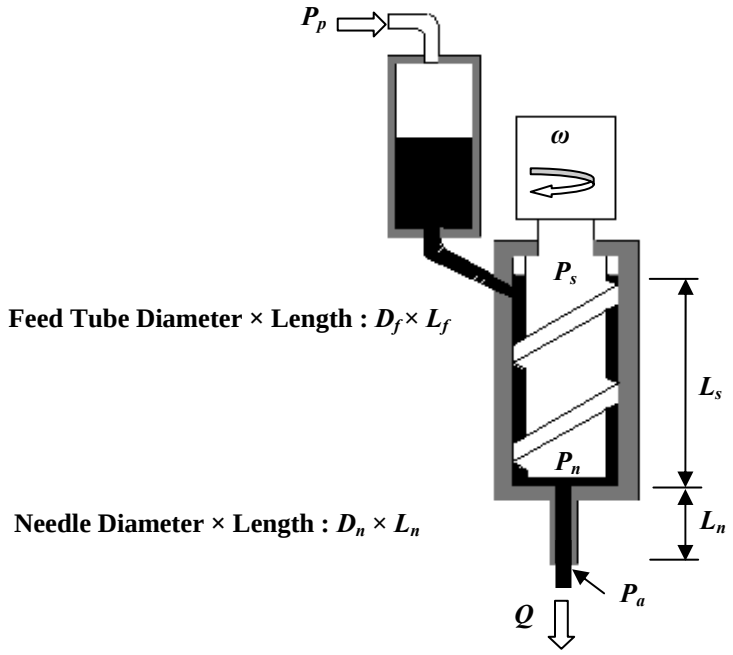

Figure 3.5. Schematic of dispensing system and the pressures of interest.

In the dispensing process, the static pressure is ignored considering the fact that it is much smaller than the operating pressure in the fluid. Therefore, the pressure gradient in the screw down channel is given by

$$g_z = \frac{(P_n - P_s)\sin\varphi}{L_s} \tag{3.25}$$

where L_s is the distance between the fluid entrance to the screw and the entrance to the needle.

As the internal diameter of the reservoir is usually much greater than that of the feed tube, the pressure drop in the reservoir due to friction can be ignored, which implies that the fluid pressure in the reservoir is uniform and equal to the applied air pressure. By taking into account the minor losses due to the effect of the entrance to the feed tube, the pressure gradient g_f in the feed tube is given by

$$g_f = -\frac{P_p - P_s - P_{mf}}{L_f} \tag{3.26}$$

where L_f is the feed tube length, and P_{mf} is the pressure drop due to the minor losses. It is given by $1.12\rho u_f^2$, in which ρ is the fluid density and u_f the average velocity of fluid in the feed tube. Similarly, the pressure gradient g_n in the needle is also given by

$$g_n = -\frac{P_n - P_a - P_{mn}}{L_n} \tag{3.27}$$

where P_{mn} is the pressure drop due to the effect of the entrance to the needle and given by $1.12\rho u_n^2$, in which u_n is the average velocity of fluid in the needle. In the above equation, the fluid pressure at the exit of the needle P_a can usually be approximated by the ambient air pressure. If the needle diameter is very small, however, the pressure difference between the fluid and the ambient air, due to the fluid surface tension, should be considered. In this case, the fluid pressure at the exit P_a can be derived based on the Laplace equation [Laplace 1806] and given by

$$P_a = P_{aa} + \frac{2\sigma}{D_n} \tag{3.28}$$

where P_{aa} is the ambient air pressure and σ is the fluid surface tension.

Combining the pressure gradients established above with the flow rate Equations (3.17) and (3.24), the expressions of the flow rate in the feed tube, the flow rate in the down screw channel, and the flow rate in the needle can be obtained, respectively. It should be noted that these expressions involve the pressures P_s and P_n, both of which are unknowns. In order to eliminate P_s and P_n and to develop an expression for the flow rate of fluid dispensed Q, one can utilize the relationship that, under the assumption that the fluid is in steady state flow, the flow rate of fluid dispensed Q is equal to the flow rate in

the feed tube, the one in the down screw channel, and the one in the needle. The equations above mentioned are summarized as

$$Q = c_1(P_p - P_{mf} - P_s)^{1/n} \tag{3.29}$$

$$Q = c_{21}\omega - c_{22}(P_n - P_s) \tag{3.30}$$

$$Q = c_3(P_n - P_a - P_{mn})^{1/n} \tag{3.31}$$

where

$$c_1 = \frac{\pi n D_f^{(3n+1)/n}}{2^{(3n+2)/n}(3n+1)(KL_f)^{1/n}}$$

$$c_{21} = \frac{(4+n)WHD_{sw}\cos\varphi}{20}$$

$$c_{22} = \frac{WH^3\sin\varphi}{4K(1+2n)L_s}\left(\frac{D_{sw}\omega\cos\varphi}{2H}\right)^{1-n}$$

$$c_3 = \frac{\pi n D_n^{(3n+1)/n}}{2^{(3n+2)/n}(3n+1)(KL_n)^{1/n}}$$

Solving for P_s and P_n in terms of Q, respectively, from Equations (3.29) and (3.31) and then substituting into Equation (3.30) yields

$$Q + \left(\frac{c_{22}}{c_3^n} + \frac{c_{22}}{c_1^n} \right) Q^n = c_{21}\omega + c_{22}(P_p - P_a - P_{mf} - P_{mn}) \tag{3.32}$$

It is seen from the above equation that the flow rate of fluid dispensed is determined by the process control parameters or dispensing conditions, i.e., ω and P_p, and also affected by the screw geometry and fluid flow behavior through the coefficients *c*s. It is also seen that the left-hand side is an increasing function of Q, implying that there is a unique solution to Q for given dispensing conditions. The solution can be obtained by employing a root finding technique, e.g., the Newton-Raphson method, to numerically solve above the equation.

For the case where the fluid being dispensed is a Newtonian one, i.e., $n = 1$, Equation (3.32) has an analytical solution, which is given by

$$Q = \frac{c_{21}\omega + c_{22}(P_p - P_a - P_{mf} - P_{mn})}{1 + \frac{c_{22}}{c_3} + \frac{c_{22}}{c_1}} \tag{3.33}$$

Correspondingly, the coefficients are reduced to

$$c_1 = \frac{\pi D_f^4}{128 K L_f},\ c_{21} = \frac{W H D_{sw} \cos\varphi}{4},\ c_{22} = \frac{W H^3 \sin\varphi}{12 K L_s},\quad \text{and}\quad c_3 = \frac{\pi D_n^4}{128 K L_n}$$

3.3. Summary

This chapter represents the development of a steady state model for the flow rate of fluid dispensed in the rotary-screw dispensing system. Under the assumption that the fluid is incompressible, the flow in screw channels and the flow in the circular tubes are examined separately, and then the flow rate of the fluid dispensed is derived.

For the flow in the screw channel, it is assumed that the syringe (barrel) is a flat plate moving on the screw channel by neglecting the channel curvature, and that the channel width is infinite. Under these assumptions, the governing equations and the boundary conditions were presented, and the solutions to them were discussed from both numerical and analytical perspectives. In particular, for the flow in the screw channel with a helix angle in the range of 15° to 25°, the flow rate inside the screw channel was developed. For the flow in the circular tubes such as needle and feed tube, based on the balance of the forces on a cylindrical element of fluid inside the circular tubes, the flow rate inside the tubes can be derived. Combining the flow rate equations given for the screw channel, the feed tube, and the needle, the flow rate of fluid dispensed is obtained by eliminating the intermediate parameters.

4. DYNAMIC MODELING OF THE FLOW RATE OF FLUID DISPENSED

4.1. Introduction

In Chapter 3, a steady state model was developed for the rotary-screw dispensing system. It was assumed that the pressure concerned in the system had reached its steady state value, and thus the effect of fluid compressibility could be neglected. This assumption is true only for dispensing large amounts of fluid with continuous rotation of screw. Thus, the model developed in Chapter 3 is not valid to describe the dynamics of the flow rate of fluid dispensed. This, however, is critical if the fluid amount required to dispense is very small. To predict the small amount of fluid dispensed in such situations, there is a need of a model, upon which the dynamics of the flow rate can be represented. This chapter is to present the development of such a dynamic model, in which the fluid compressibility is considered.

Generally, the development of the model for the dynamics of the flow rate in the rotary-screw dispensing system consists of three steps: 1) representing the dynamics of the flow rate in the syringe, 2) representing the dynamics of the flow rate in the needle, and 3) representing the dynamics of the flow rate of the fluid dispensed. These are discussed in detail in the following sections.

4.2. Dynamic Modeling of the Flow Rate in the Syringe

A schematic of the rotary-screw dispensing system considered in this study is repeated in Figure 4.1. As it was mentioned previously, the syringe is assumed to be unwrapped as a flat plate and that the flat plate moves over the flat rectangular channel. It is also assumed in this chapter that (1) the fluid in the syringe is compressible, (2) the fluid flow behavior is non-Newtonian, (3) the pressure inside the syringe is linearly distributed down the channel, and (4) there is no slip between the fluid and the syringe wall, and (5) the friction losses are neglected.

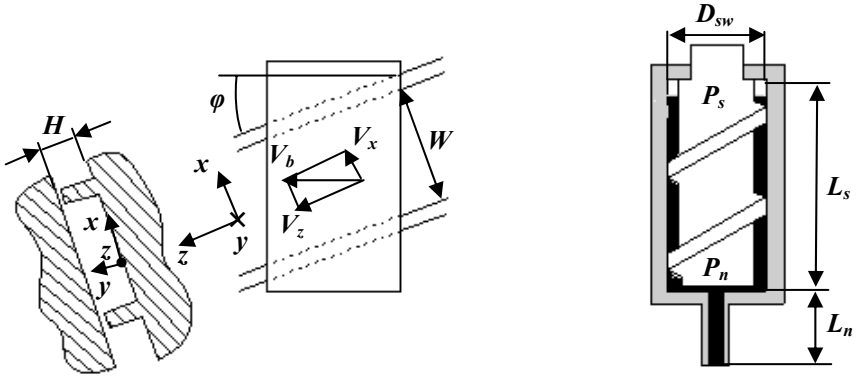

Figure 4.1. Geometry of the rotary-screw and the syringe.

From the preceding chapter, it is known that the flow rate out of the syringe is a combination of the drag flow and the pressure-driven flow. This is also applicable if the

dynamics of the flow rate is considered. Therefore, the general form of the flow rate can be presented as

$$Q = C_\omega \omega - Q_P \tag{4.1}$$

where Q is the flow rate out of the syringe, Q_p is the pressure-driven flow rate, ω is the rotation speed of the screw, and C_{ω} is the coefficient associated with the pure drag flow.

If the fluid in the syringe is compressible, as assumed previously, using the bulk modulus, B, to measure the fluid compressibility, one has

$$\frac{1}{B} = -\frac{1}{V_f}\frac{\mathrm{d}V_f}{\mathrm{d}P} \tag{4.2}$$

where V_f denotes the fluid volume inside the syringe and P the pressure inside the syringe.

It is noted that Equation (4.2) is valid only if the pressure in the syringe is uniformly distributed. However, as a fact, the pressure in the syringe is linearly distributed down the screw channel. To deal with this situation, it is proposed to use the average pressure in the syringe in this study. Thus, Equation (4.2) needs to be modified by using the average pressure, $(P_n\text{-}P_s)/2$, in which P_n and P_s are the fluid pressure at the bottom and top of the screw channel, respectively. This modification leads to, assuming that P_s is a constant during the dispensing process.

$$\frac{1}{B} = -\frac{1}{V_f}\frac{\mathrm{d}V_f}{\frac{\mathrm{d}P_n}{2}} \tag{4.3}$$

From the above equation, the rate of volume change in syringe can then be related to P_n, by differentiating the above equation as

$$Q_c = -\frac{V_f}{2B}\frac{\mathrm{d}P_n}{\mathrm{d}t} \tag{4.4}$$

where Q_c denotes the rate of volume change in syringe due to the fluid compressibility. The net pressure-driven flow rate is then given by

$$Q_p = \frac{V_f}{2B}\frac{dP_n}{dt} + C_p(P_n - P_s) \tag{4.5}$$

where C_p is the coefficient associated with the pure pressure-driven flow, as derived in the preceding chapter.

Substitution of Equation (4.5) into the Equation (4.1) results in

$$C_\omega \omega - Q = \frac{V_f}{2B}\frac{dP_n}{dt} + C_P(P_n - P_s) \tag{4.6}$$

Particularly, C_ω and C_p can be given by

$$C_\omega = \frac{(4+n)WHD_{sw}\cos\phi}{20} \quad \text{and} \quad C_p = \frac{WH^3}{(1+2n)4\mu L_s} \tag{4.7}$$

4.3. Dynamic modeling of the flow rate in the needle

To represent the flow rate in the needle as illustrated in Figure 4.2, it is assumed that (1) the fluid in the needle is incompressible which is reasonable considering that the fluid volume in the needle is small relative to that in the syringe, (2) the fluid behavior is non-Newtonian time-independent, (3) the flow is laminar and fully developed, and (4) there is no slip between the fluid and the needle wall. Under these assumptions, considering the fluid in a vertical annular element with the needle length L_n and the radial thickness dr at a radius r, the summation of forces acting on the annular element of the fluid is given by Chen et al**.** [2002] as

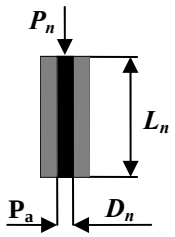

Figure 4.2. Schematic of pressure-driven flow in the needle.

$$2\pi r dr\Delta P + \sum F_{shear} = 2\pi r dr L_n \rho \frac{\partial u}{\partial t} \tag{4.8}$$

where

$$\sum F_{shear} = 2\pi r dr L_n (r\frac{\partial \tau}{\partial r} + \tau) \tag{4.9}$$

Substituting the Equaiton (4.9) in to the Equation (4.8) and simplifying it results in

$$\frac{\Delta P}{L_n} + \frac{\partial \tau}{\partial r} + \frac{\tau}{r} = \rho \frac{\partial u}{\partial t} \tag{4.10}$$

where ΔP is the pressure drop in the needle ($\Delta P = P_n - P_a$ in which P_n and P_a denote the pressures at the needle inlet and the needle outlet respectively), ρ is the fluid density, L_n is the needle length, τ is the shear stress in fluid and u is the fluid average velocity. In this equation, the first term of the left side is the force due to the pressure drop ΔP, and the second term is the forces acting on inside and outside surface of the fluid cylindrical element resulting from fluid viscousness.

To solve the above equation, the relationship between the shear stress and the shear rate in the fluid is needed. This relationship can be either linear for Newtonian fluids or non-linear for non-Newtonian fluids. The substitution of the non-Newtonian relationship into the equation of force equilibrium inside the needle, Equation (4.10), makes the equation very complicated. To avoid the complexity, the fluid is assumed to be Newtonian. For Newtonian fluids, the relationship between the shear stress and the shear rate is given by $\tau = K\dot{\gamma}$, in which K is the fluid viscosity and $\dot{\gamma}$ is the shear rate in the

fluid. Solving the above equation, the transfer function of the flow rate to the applied pressure was given by [Chen et al. 2002 and 2003].

$$Q(s)/\Delta P(s) = \frac{Q_u}{\rho L_n Q_u / A_n s + 1} \tag{4.11}$$

where L_n and A_n are the length and cross-sectional area of the needle respectively, and Q_u is the steady state flow rate under a unit pressure, depending on the fluid behavior and the needle geometry.

It can be seen that for Newtonian fluids the dynamics of the flow rate to the pressure drop is equivalent to a first-order system, in which the steady state value depends on Q_u, and the time constant depends on both the inertia of the fluid in the needle (ρL_n) and the steady state average velocity (Q_u/A_n).

To take non-Newtonian behavior into account, the flow rate dynamics for non-Newtonian fluids is assumed to have the same form as Newtonian fluids given in Equation (4.11). The influence of the non-linear relationship between the shear stress and the shear rate on the flow rate dynamics is included by modifying the steady state flow rate Q_u. Therefore, for the fluids whose behaviors are characterized by the "Power Law" equation in Equation (4.11), Q_u is given by [Chen et al. 2002]

$$Q_u = \frac{n\pi R^3}{3n+1}\left(\frac{\tau_w}{K}\right)^{1/n} \tag{4.12}$$

where τ_w is the shear stress at the needle wall under the applied pressure. Taking into account the minor losses of energy due to the effect of the needle entrance and exit, τ_w is

$$\tau_w = \frac{D_n}{4L_n}(P_n + L_n \rho g - 1.12\rho u^2) \tag{4.13}$$

where g is the acceleration due to gravity, and u is the average velocity of the fluid in the needle.

4.4. Dynamic Modeling of the Flow Rate of the Fluid Dispensed

Based on the flow rates of fluid in the syringe and needle, established in the previous sections, a model is presented in this section to represent the dynamics of the flow rate of fluid dispensed in the rotary-screw dispensing process. It is noted that the dynamics of the flow rate may involve the dynamics of the flow in the feed tube, the flow in the screw channel, and the flow in the needle. To simplify the presentation, it is assumed in this section that the dynamics of the flow in the feed tube is not involved by properly controlling the dispensing system, for example, applying the pressurized air at a right time moment prior to the screw rotation such that a steady state flow in the feed tube rate can be established before dispensing.

Taking the Laplace transformation of Equation (4.6) and combining with Equation (4.11) results in the removal of the intermediate parameter P_n. Therefore, the transfer function of the system can be derived as

$$\frac{Q(s)}{\omega(s)} = \frac{C_\omega}{a_2 s^2 + a_1 s + (\frac{C_p}{Q_u} + 1)} \tag{4.14}$$

where

$$a_2 = \frac{\rho L_n V_f}{2\beta A_n} \quad \text{and} \quad a_1 = \frac{V_f A_n + 2\beta C_p \rho L_n Q_u}{2\beta Q_u A_n} \tag{4.15}$$

It can be seen that the dynamics of the flow rate of fluid dispensed to the rotation speed of the screw is a second order system, in which the transient response depends on the parameters such as the fluid properties and the geometries of both screw and needle.

4.5. Summary

In the rotary-screw dispensing process, the flow rate dynamics is an important parameter, which is particularly true if the amount of fluid required to dispense is very small. This chapter presents the development of a dynamic model. In particular, the dynamics of the flow rate in the syringe and needle is presented, by taking into account the fluid flow behavior, compressibility, and inertia; on this basis, a model to represent the dynamics of the flow rate of fluid dispensed in the rotary-screw dispensing process is developed. Based on the model developed, it is seen that the dynamics of the flow rate of fluid dispensed to the rotation speed of the screw is equivalent to the second order system, in which the transient response is characterized by the fluid flow behavior, the geometry of the screw, and the geometry of the needle.

5. EXPERIMENT AND SIMULATION RESULTS

In this study, two models were developed for the rotary screw dispensing system; one model is for the steady flow rate of fluid dispensed, as presented in Chapter 3, and the other one is for the unsteady flow rate, as presented in Chapter 4. This chapter is to present the experiments and results for the model validation, as well as the simulations that have been carried out based on the models. The simulation programs are presented in appendices.

5.1 Experimental Setting

The experiments of dispensing fluid presented in this chapter were all conducted on a typical commercial dispensing system of DS 500 (provided by Assembly Automation Limited, Hong Kong). A schematic of the overall system and a close up view of the dispensing head and chuck are shown in Figures 5.1(a) and 5.1(b), respectively. In this system, the dispensing head carries the dispensers to move in three directions, and the chuck holds the substrates or boards on it using a vacuum method. The system temperatures can be controlled with a resolution of ±1 ºC. In the experiments, pressurized air was provided by an air supply of ∑- MX 9000 SM II with a resolution of 1 kPa; and a rotary-screw dispenser of TS 5000 was used to deliver the fluid Hysol EO 1062, which is a typical encapsulant used in electronic packaging. The values of the

geometrical parameters and the dispensing conditions used in the experiments are listed in Table 5.1 except where specified.

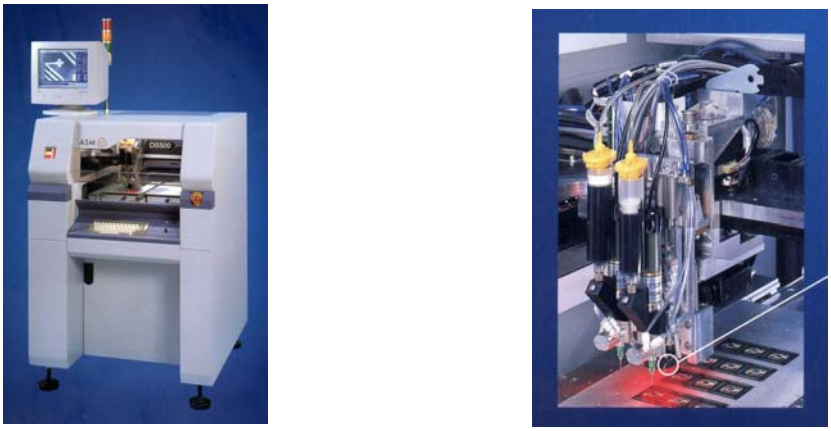

(a) (b)

Figure 5.1. DS 500 dispensing system: a) overall system and b) dispensing head and chuck.

Table 5.1. Geometrical parameter values and the dispensing conditions.

	Parameters	Values
Geometry	**Screw outer diameter, D_{sw}**	**3.40 mm**
	Screw channel width, W	**3.266 mm**
	Screw channel depth, H	**0.57 mm**
	Screw helix angle of the screw, φ	**17 degrees**
	Needle diameter, D_n	**0.8382 mm**
	Needle length, L_n	**25.4 mm**
	Feed tube diameter, D_t	**3.0 mm**
	Feed tube length, L_t	**50.0 mm**
	Distance from the entrance of the screw to the entrance of the needle, L_s	**16.0 mm**
Dispensing Conditions	**Screw rotational speed, ω**	**43.96 rad/s**
	Applied air pressure, P_p	**2.0×10^5 Pa**
	System temperature, T	**60 °C**

5.2. Results Related to the Characterization of Flow Behavior

As discussed in Chapter 2, basically there are two methods to determine the parameters of the model used for the flow behavior characterization, i.e., the use of a rheometer and the determination from dispensing experiments. The use of a rheometer is a common method, and the applications of the so-characterized fluid properties require that the temperature in the dispensing process in this study be controlled as same as the one in the rheometer. Otherwise, a little difference between them can result in a significant error [Chen and Ke 2005]. Instead of using a rheometer, in this study the fluid flow behavior was identified and characterized from the results obtained from a few dispensing experiments. For this purpose, the dispensing system described previously was controlled to dispense fluid for a specific time period of 100 seconds at different dispensing conditions. At each of the dispensing experiments, the average flow rate was measured by weighing the dispensed fluid amount using an electronic balance with a resolution of 0.01 mg. The measured flow rates are given in Table 5.2, along with the dispensing conditions used.

Table 5.2. Measured flow rates at different dispensing conditions.

Experiments	Applied air pressure ($\times 10^5$ Pa)	System temperature (°C)	Measure flow rate (mg/s)
1	1.0	60	37.60
2	2.0	60	39.68
3	3.0	60	43.14
4	4.0	60	46.41
5	3.0	40	36.62
6	3.0	80	50.42

To characterize the fluid flow behavior, the power law equation given by $\tau = K\dot{\gamma}^{n}$ was used. K was fitted as a function of temperature to account for the temperature influence on the flow behavior. In particular, the function takes the following form,

$$K = K_{\circ} e^{T_k / T} \tag{5.1}$$

where T is the system temperature with a unit of ºC and $K_{\circ}$ and T_k are parameters to be identified, with units of Pa·s and ºC, respectively. Using the measured flow rate given in Table 5.2, the values of the parameters, i.e., n, $K_{\circ}$ and T_k, were identified based on the steady state model developed in Chapter 3. These parameters are alternatively changed in the model until the flow rates obtained from the steady state model are in minimum distance from the measured flow rates out of experiments. In particular, the function of nonlinear least-squares regression in Matlab was used to estimate the parameter values. This function estimates the parameters by starting with an initial guess and then altering the guess until the algorithm converges. By doing so, n, $K_{\circ}$ and T_k are given the value of 0.994, 1.446 Pa·s, 146.23 ºC, respectively.

5.3. Results Related to the Steady state Model

To verify the effectiveness of the steady state model developed in Chapter 3, dispensing experiments were conducted again by using the dispensing conditions, which

were different from those used in the experiments conducted previously for the flow behavior characterization. Specifically, the fluid was dispensed by applying the air pressure of 1, 2, 3, and 4 bar at the system temperature of 40, 60, 80 ºC, respectively. As in the previous experiments, the average flow rates were measured by weighing the dispensed fluid amount, which are given in Figure 5.2.

Based on the steady state model developed, simulations were carried out to predict the flow rate of fluid dispensed by using the flow behavior identified from the previous experiments. The simulation results are shown in Figure 5.2 in solid lines for the comparison with the experimental ones. It can be seen that the model predictions are in close agreement with the measured values, which indicates that the model developed in this study is promising to be used for the flow rate prediction in the rotary screw dispensing process.

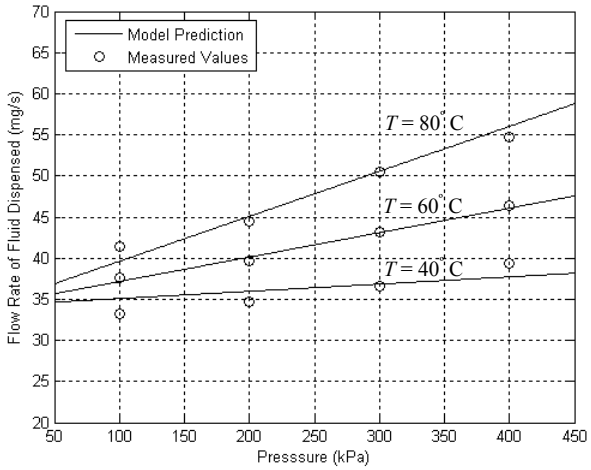

Figure 5.2. Flow rate vs. applied air pressure at different temperatures.

In order to gain insight into the performance of the rotary screw dispensing process, some more simulations were carried out based on the steady state model. The objective is to identify the effects of the flow behavior, the applied air pressure, the system temperature, and the needle diameter on the relationship between the flow rate of fluid dispensed and the screw rotational speed. These effects are essential to set up a dispensing process, by rationally choosing the dispensing conditions rather than using trial and error, for a particular dispensing application. In all of the simulations, the values of the geometrical parameters and the dispensing conditions given in Table 5.1 and the flow behavior identified previously were used.

The first simulation result given in Figure 5.3 shows the relationship between the flow rate and the screw speed at different values of the power law index n, which correspond to different fluid materials. It indicates that the flow rate increases as the screw speed increases for all values of n. If the fluid is Newtonian (i.e., $n = 1$), the flow rate increases linearly. For non-Newtonian fluids (i.e., $n \neq 1$), the flow rate increases non-linearly with the screw speed; specifically, at the lower screw speed, the flow rate increases with the screw speed much faster than that at the higher screw speed.

The second simulation result in Figure 5.4 illustrates the relationship between the flow rate and the screw speed at different values of the applied air pressure P_p. It is seen that the larger applied air pressure results in the larger flow rate.

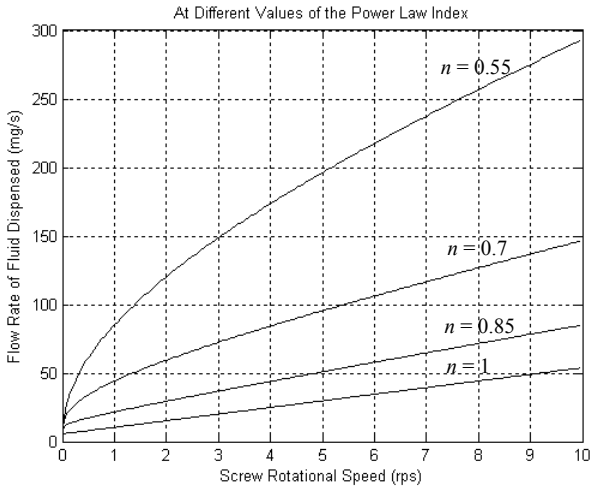

Figure 5.3. Flow rate vs. screw speed at different power law index, n.

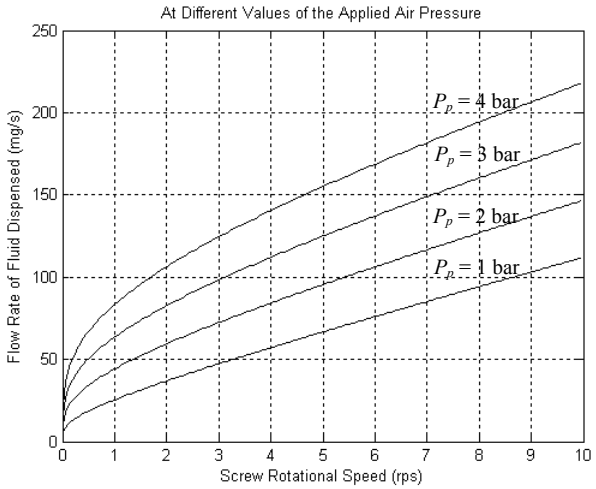

Figure 5.4. Flow rate vs. screw speed at different applyied air pressures, P_p.

The third simulation result in Figure 5.5 shows the relationship between the flow rate and the screw speed at different values of the system temperature. The result indicates that the higher system temperature can result in the larger flow rate.

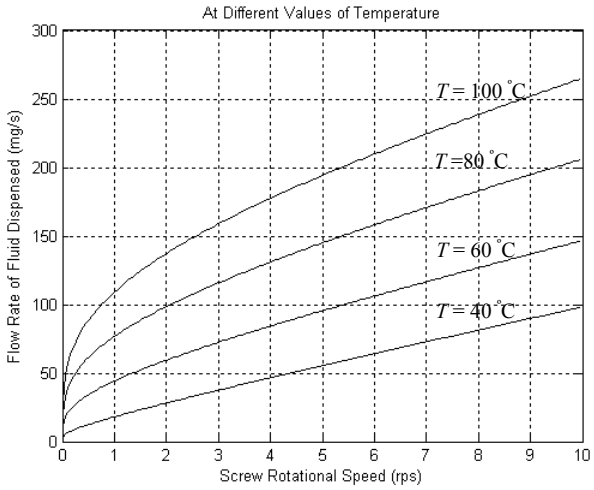

Figure 5.5. Flow rate vs. screw speed at different system temperatures, T.

The fourth simulation result in Figure 5.6 shows the relationship between the flow rate and the screw speed at different values of the needle diameter, indicating that the bigger needle diameter can result in the larger flow rate.

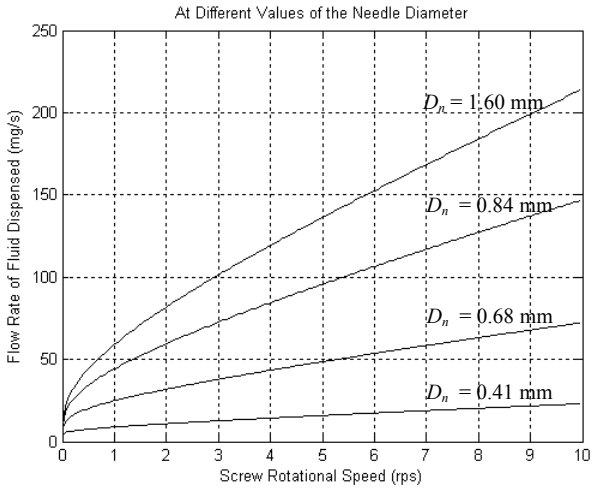

Figure 5.6 Flow rate vs. screw speed at different needle diameters, D_n.

5.4. Results Related to the Dynamic Model

This section presents an investigation, based on the dynamic model presented in Chapter 4, into the performance of the rotary-screw dispensing process. The main objective is to identify the influence of the dispensing time, the needle temperature, the fluid behavior, and the fluid compressibility on the consistency in amount of fluid dispensed. The values of the geometrical parameters, the dispensing conditions, and the flow behavior parameters used in this investigation are the same as those used in previous sections.

In dispensing small amounts of fluid, the actual amount of fluid dispensed is different from the design amount due to the dynamics of the flow rate. The design amount is given in terms of the steady state flow rate, i.e., $\rho Q_s T_d$ where Q_s is the steady state flow rate and T_d is the dispensing time period. The actual amount of fluid dispensed is evaluated based on the dynamics of the flow rate, specifically simulated by using $\rho \int Q dt$. To measure the difference between the actual amount and the design amount of fluid dispensed, a relative error is used in this study, which is defined in the following equation.

$$Error = \frac{\rho \int Q dt - \rho Q_s T_d}{\rho Q_s T_d} \times 100\% \tag{5.2}$$

In the first simulation, the flow rate was simulated using different values of the dispensing time T_d. Figure 5.7 demonstrates the results for T_d = 0.001, 0.003, 0.010, and

0.045 S. The results indicate that for a small value of T_d, the flow rate can not reach its steady state value. In other words, in transient response, the dynamics of the flow rate is very important and is not equal to the steady state value of the flow rate. Figure 5.8 represents the calculated relative errors at different values of T_d. It suggests that, as T_d increases, the error decreases and approaches zero, implying that the influence of the flow rate dynamics can be ignored.

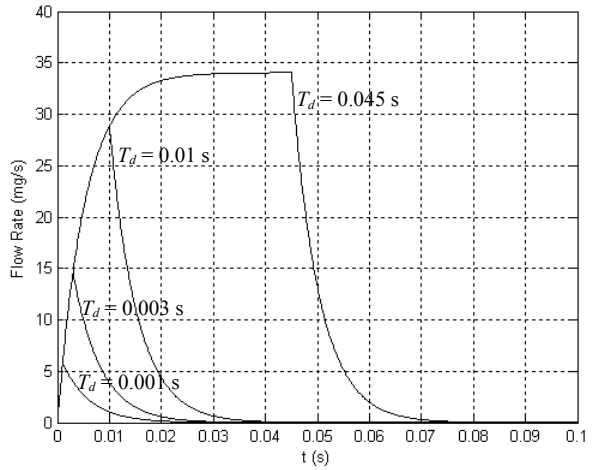

Figure 5.7. Influence of the dispensing time on the flow rate.

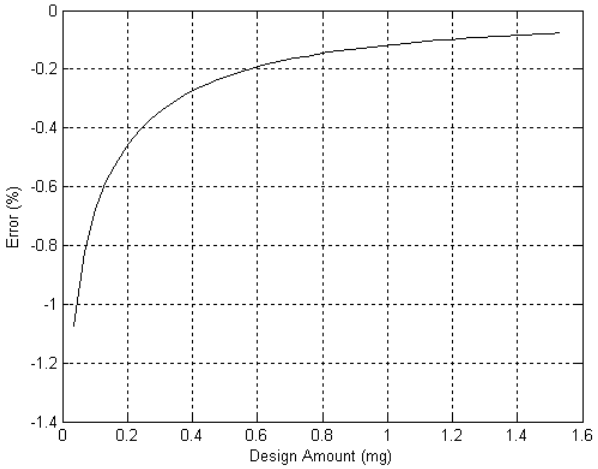

Figure 5.8. Relative errors vs. the design amounts.

The second simulation is to investigate the effect of the needle temperature on the consistency in amount of fluid dispensed, while the other parameters are fixed. Figures 5.9 and 5.10 illustrate the response of the flow rate and the relative error for different temperatures T = 27, 35, and 45 ºC, respectively. It is seen that changing the needle temperature significantly affects the fluid characterizations represented by K, which is function of the temperature and thereby the flow rate and the consistency in the amount of fluid dispensed. In other words, the higher the temperature, the faster the transient response of the flow rate, and the lower the inconsistency in the amount of the fluid dispensed can be resulted.

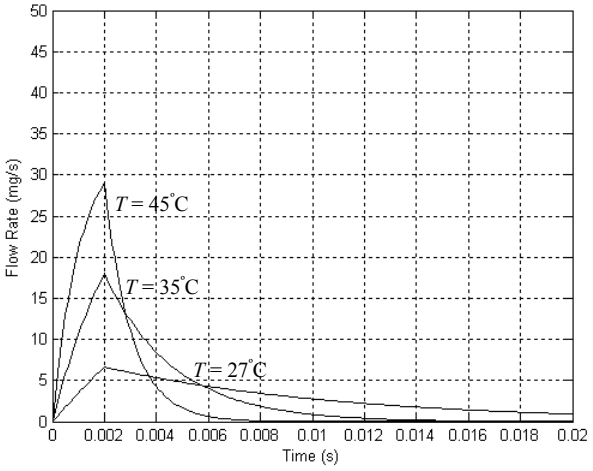

Figure 5.9. Influence of the needle temperature on the flow rate.

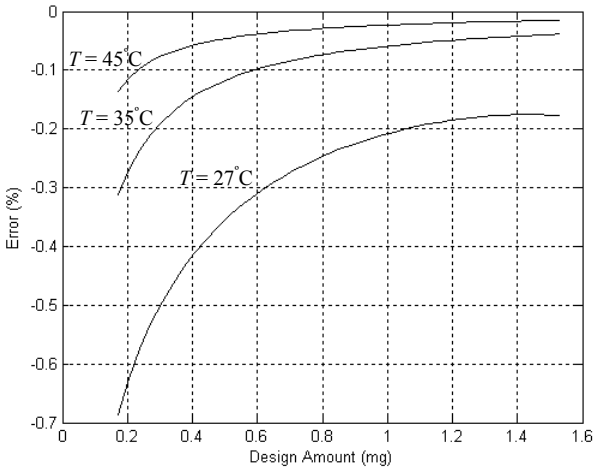

Figure 5.10. Relative errors vs. the design amounts with different temperatures, *T*.

The third simulation is to investigate the effect of fluid compressibility on the consistency in amount of fluid dispensed, while the other parameters are fixed. Figure 5.11 and 5.12 illustrate the response of the flow rate and the relative error for different values of B = 0.8e9, 1e9, and 5e9 Pa, respectively. It is seen that the fluid compressibility can change the dynamics of the flow rate, and thereby the consistency in the amount of fluid dispensed. In other words, the more pronounced the fluid compressibility, the slower the transient response of the flow rate, and the more pronounced inconsistency in the dispensing process can be resulted.

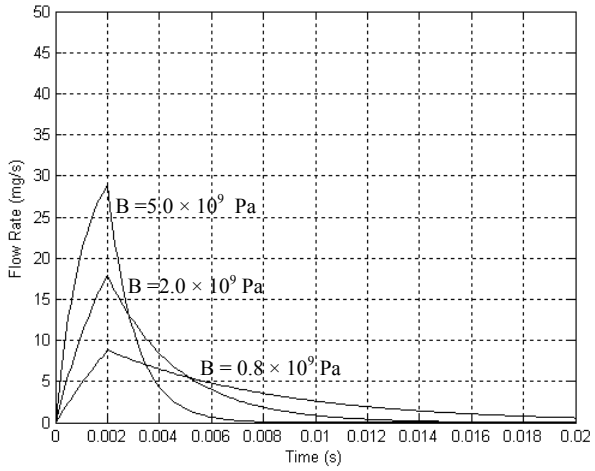

Figure 5.11. Influence of the fluid compressibility on the flow rate.

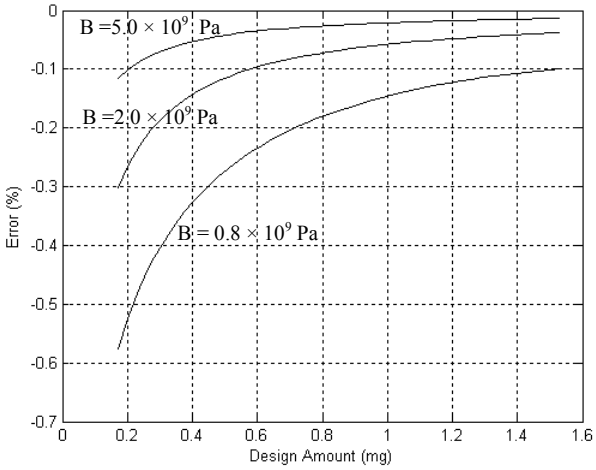

Figure 5.12. Relative errors vs. the design amounts with different *B* values.

The fourth simulation is to investigate the effect of fluid flow behavior on the consistency in amount of fluid dispensed. The difference in fluid behavior can be represented by using different values of the parameters of *n*, and *K* in Equation (2.1). In this simulation, different values of *n* were used. Figures 5.13 and 5.14 illustrate the

response of the flow rate and the relative error for different values of n = 0. 5, 0.85, and 0.95 respectively. It is seen that, the greater departure of n from unity, the more non-Newtonian behavior, the faster the transient response of the flow rate, and the more pronounced inconsistency in the fluid volume dispensed can be resulted.

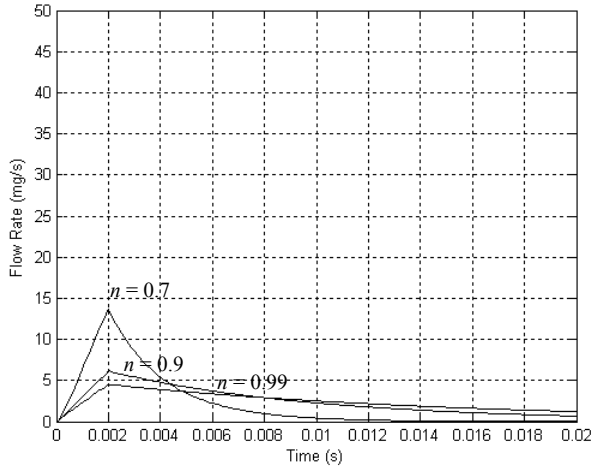

Figure 5.13. Influence of the non-Newtonian behavior on the flow rate

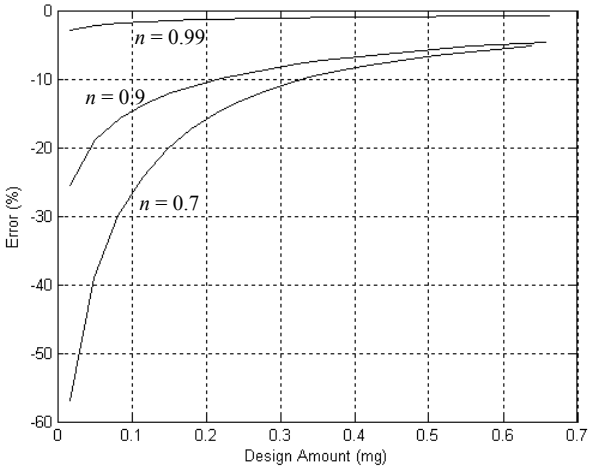

Figure 5.14. Relative errors vs. the design amounts with different n values.

5.5. Summary

This chapter presents the experiment and simulation results related the models developed in chapters 3 and 4. The experiments were conducted on a typical commercial dispensing system of DS 500 (provided by Assembly Automation Limited, Hong Kong). At first, the fluid flow behavior was identified by using the results obtained from a few dispensing experiments. Then, the effectiveness of the steady state model was investigated experimentally. The results shows that the steady state model predictions are in close agreements with the measured values, indicating that the model developed is promising to be used for the flow rate prediction in the rotary-screw dispensing process.

Based on the steady state model, the simulations were carried out to identify the effects of the flow behavior, the applied air pressure, the system temperature and the needle diameter on the relationship between the flow rate of fluid dispensed and the screw rotational speed. Based on the dynamic model, the simulations were also carried out. The objective was to investigate the inconsistency in the amount of fluid dispensed, resulted from the difference in fluid compressibility and flow behavior and the difference in the needle temperature. It has been shown that the lower the needle temperature, the higher the fluid compressibility, the more pronounced non-Newtonian behavior, the more pronounced inconsistency in the fluid volume dispensed can result.

6. INTEGRATED MODELING AND DESIGN APPROACH FOR ROTARY-SCREW DISPENSING SYSTEMS

6.1. Introduction

There are various methods developed in literature to model and control the three categories of dispensing systems shown in Figure 1.2 in order to improve their dispensing performances [Chen et al. 2002 and 2003, Hong and Li 2003]. However, there is a lack of approach that allows the designers and users to systematically evaluate and compare the three categories of dispensing systems in terms of their dispensing performances. Obviously, the capability of doing so would be of great advantage to the designers when developing new dispensing systems, and to the users when choosing a proper dispensing system for their specific applications. This chapter is to present the development of such an approach based on the principles of axiomatic design.

6.2. Axiomatic Design

Axiomatic design is one of the most powerful design approaches and has been used in various engineering design processes such as the design of software, manufacturing

systems, materials and products. The two fundamental principles of axiomatic design, i.e., the independence axiom and the information axiom, are briefly described as follows.

6.2.1. Independence Axiom

In the axiomatic approach [Suh 2001], the design process is defined as the mapping between the functional requirements (FRs) and the design parameters (DPs). The FRs are the minimum set of independent requirements that completely characterizes the functional needs of the product/system that needs to be designed. The DPs are the physical variables, which characterize the design that satisfies the specified FRs. Generally, the mapping between FRs and DPs can be expressed mathematically as

$$\{FR\} = [A]\ \{DP\} \tag{6.1}$$

where [A] is the design matrix, which characterizes the product/system design, and defines the relationship between FRs and DPs and is given by

$$[A] = \begin{vmatrix} A_{11} & A_{12} & \dots & A_{1n} \\ \vdots & \vdots & \vdots & \vdots \\ A_{m1} & A_{m2} & \dots & A_{mn} \end{vmatrix} \tag{6.2}$$

where the element A_{ij} is the sensitivity of FR_i to DP_j or $A_{ij} = \partial FR_i / \partial DP_i$, which could be determined by means of either the model of the product/system or the designer's knowledge on the product/system, if the model is not available. If A_{ij} is constant, the design is said to be linear. Otherwise, it is a non-linear design.

The independence axiom states that the FRs must always be maintained independent of one another by choosing appropriate DPs. To satisfy the independence axiom, the design matrix [A] should be either diagonal or triangular. If the design matrix is diagonal, each FR can be satisfied independently by means of one DP, and such a design is called an uncoupled design. If the design matrix is triangular, the independence of FRs can be guaranteed only if the DPs are determined in a proper sequence, and such a design is called a decoupled design. Any other form of the design matrix does not meet the independence axiom, and the result is called a coupled design. Therefore, if several FRs must be satisfied, the design should be carried out such that either a diagonal or a triangular matrix can be resulted.

6.2.2. Information Axiom

For a design task defined by a given set of FRs, it is possible that different designs can be resulted, all of which may be acceptable in terms of the independence axiom. However, one of these designs is likely to be the best one. The information axiom is used to provide a quantitative measure of the merits of a given design such that the best design can be determined among the different ones. In particular, the information axiom

[Suh 2001] states that, among the designs that are equally acceptable from the functional point of view, the design with the minimum information content is the best design.

The information content of a given design is defined in terms of the probability of satisfying the given set of FRs. Generally, in the case of n FRs, the information content *I* is given by

$$I = -\sum_{i=1}^{n} \log_2 P_{i\{j\}} \qquad \{j\} = \{1,2,.....,i-1\} \tag{6.3}$$

where $\log_2$ is the base-2 logarithm with unit of bit, $P_{i\{j\}}$ is the conditional probability of the satisfying FR_i, given that all other relevant or correlated $\{FR_j\}_{j=1,2,...i-1}$ are also satisfied.

The probability of satisfying a FR can be evaluated by specifying the design range for the FR and determining the system range that the proposed design can provide to satisfy the FR. Figure 6.1 presents the two mentioned ranges graphically, in which the vertical axis represents the probability distribution density PDF, and the horizontal axis represents FR.

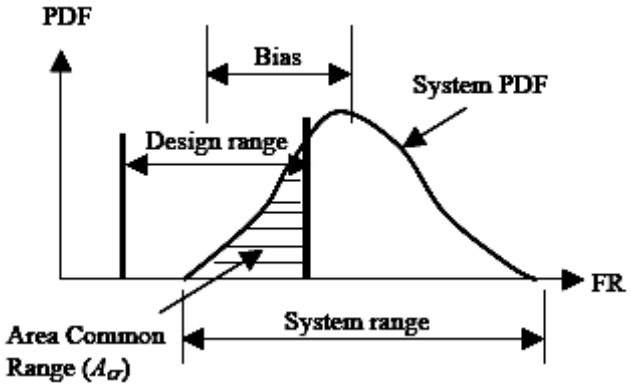

Figure 6.1. Design range, system range, common range, and the system PDF of a FR [Suh 2001].

The common or overlap range between the design range and the system range specify the region where the FR is satisfied. Therefore, the area under the system PDF within the common range, A_{cr}, represents the probability of achieving the FR. If all FRs are satisfied independently, as are the cases for the decoupled and uncoupled designs, Equation (6.3) can also be rewritten as:

$$I = \sum_{i=1}^{n} \log_2 (1/A_{cr}) \tag{6.4}$$

For a design, if the system range falls completely within the design range for each of the FRs, then each A_{cr} is equal to one, and the information content is zero.

6.3. Integrated Modeling and Design for the Rotary-Screw Dispensing System

As the axiomatic approach is processed in the conceptual or system level, a primitive or approximate model is sufficient to be used in the design process. Thus, the model developed in the preceding chapter is simplified in this section by assuming that the fluid being dispensed is Newtonian, and then used in the development of approach for integration of the model and design of the rotary-screw dispensing system.

6.3.1. Simplified Model for the Rotary-Screw Dispensing System

The model developed in the preceding chapter is simplified here for Newtonian fluids. For this purpose, Equation (4.6) related to the flow rate of fluid dispensed is given here again, i.e.,

$$C_\omega \omega - Q = \frac{V}{2B}\frac{dP_n}{dt} + C_P(P_n - P_s) \tag{6.5}$$

Particularly, C_ω and C_p for Newtonian fluid are given by

$$C_\omega = \frac{WHD_{sw}\cos\phi}{4} \qquad \text{and} \qquad C_p = \frac{WH^3}{12\mu L_s} \tag{6.6}$$

Combining Equation (4.11) (transfer function of the flow rate to the applied pressure in the needle) with Equation (6.5) in its Laplace form yields the transfer function of the flow rate to the rotation speed of the screw, i.e.,

$$\frac{Q(s)}{\omega(s)} = \frac{C_\omega}{a_2 s^2 + a_1 s + (\frac{C_p}{Q_u} + 1)} \tag{6.7}$$

where

$$a_2 = \frac{\rho L_n V}{2\beta A_n} \quad \text{and} \quad a_1 = \frac{VA_n + 2\beta C_p \rho L_n Q_u}{2\beta Q_u A_n} \tag{6.8}$$

Neglecting the effect of the fluid inertia in the needle gives $a_2 = 0$. Thus, Equation (6.7) can be simplified as

$$\frac{Q(s)}{\omega(s)} = \frac{C_\omega}{\frac{V}{2BQ_u} s + (\frac{C_p}{Q_u} + 1)} \tag{6.9}$$

The flow rate in the needle, Q_n, for Newtonian fluids can be obtained using the well-known "Poiseuille Equation" as

$$Q_n = \frac{\pi D_n^4 (P_n - P_a)}{128 \mu L_n} \tag{6.10}$$

where P_n is the fluid pressure at the needle entrance, P_a is the ambient pressure at the needle exit, D_n and L_n are the inner diameter and length of the needle, respectively, and μ is the viscosity of the fluid in the needle.

To substitute in Equation (6.9), Q_u is given by

$$Q_u = \frac{\pi D_n^4}{128 \mu L_n} \tag{6.11}$$

It should be noted that the flow rate in Equation (6.10) is a dynamic parameter, because the pressure P_n is a dynamic response to the manipulated parameter, as shown in Equation (6.5). Once the pressure reaches its steady state value, the flow rate obtained from the above equation is the steady state value.

Once the flow rate of fluid dispensed is known, the amount of fluid dispensed, M, can be obtained by means of the following integration

$$M = \rho \int_0^{T_d} Q dt \tag{6.12}$$

where ρ is the density, and T_d is the time period of dispensing, which depends on the duration of the screw rotation in the rotary-screw dispensing system.

6.3.2. Integrated Modeling and Design Approach

The functional requirements of the dispensing system may vary from one application to another. For continuous dispensing, such as die encapsulation shown in Figure 1.1(a), the steady state flow rate of the fluid must be well controlled in order to achieve the desired profile of the dam and the desired amount of the fluid filling the inside of the dam, while for the discontinuous dispensing, such as surface mount technology shown in Figure 1.1(b), the amount of fluid must be controlled precisely to secure the component with high degrees of quality and reliability. Based on the above considerations, in this study the functional requirements of the dispensing system are defined as controls of both the steady state flow rate and the amount of fluid dispensed by

FR_1 = steady state flow rate of the fluid dispensed, Q_s

FR_2 = amount of the fluid dispensed, M

For the rotary-screw dispensing approach, the design parameters of the dispensing system are considered as the magnitude and duration of the control action, i.e. the screw rotation by

DP_1 = magnitude of the control action, M_c

DP_2 = duration of the control action, T_d

Based on the model presented in the preceding section, the mapping between the FRs and DPs can be established for the dispensing system, and given by

$$\begin{Bmatrix} Q_s \\ M \end{Bmatrix} = \begin{vmatrix} A_{11} & 0 \\ A_{12} & A_{22} \end{vmatrix} \begin{Bmatrix} M_c \\ T_d \end{Bmatrix} \tag{6.13}$$

where the zero element represents the steady state flow rate Q_s being independent of the duration of the control action T_d. The element A_{11} is evaluated when the pressure in the fluid at the bottom of the syringe, P_n, reaches its steady state value. It can be derived from the model presented in the preceding section and given by

$$A_{11} = \frac{C_\omega}{1 + \dfrac{C_p}{Q_u}} \tag{6.14}$$

There are no closed-form expressions for the elements A_{21} and A_{22} due to the non-linearity involved. From Equation (6.13), it is seen that the design matrix is triangular, which indicates that the dispensing system has a decoupled design.

It is important to note that the elements A_{11}, A_{21}, and A_{22} in the design matrix depend on the fluid viscosity μ and the fluid volume in the syringe. In a dispensing process, the elements of $A_{11}, A_{21},$ and A_{22} are not constant, but vary due to the instability of the system temperature, which affects the fluid viscosity in the syringe. This causes the steady state flow rate and the amount of fluid dispensed to deviate from the desired values. In

accordance with the definition of information content in the axiomatic design reviewed previously, the design range, system range, and information content for a dispensing system are defined in Figure 6.2, in which the distribution of the design amount and system range are assumed to be uniform.

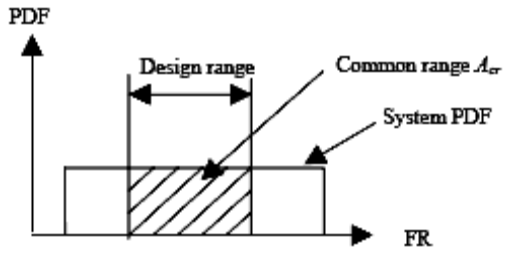

Figure 6.2. An illustration of the design range, system range, common range, and system PDF of a FR for a dispensing system.

Design range of FR_1 = desired Q_s and its tolerance

Design range of FR_2 = desired M and its tolerance

System range of FR_1 = deviation of Q_s due to the change in μ, or V_f

System range of FR_2 = deviation of M due to the change in μ, or V_f

Information content $I = \log_2(1/A_{cr})$

Based on the above definitions, the information content for each FR can be evaluated, and then by summing them up, the total information content can be obtained for the rotary-screw dispensing system. If the same procedure is applied to different dispensing systems, it allows designers and users to determine which system is the best design by

means of the information axiom. In addition, it should be noted that the approach presented in this chapter can also be applied in the design and development of the new dispensing systems.

6.4. Comparison of the Existing Dispensing Systems

To compare rotary-screw dispensing system with the other two dispensing approaches (i.e., time-pressure and positive-displacement dispensing systems), a case study is carried out to evaluate the information content of the three different systems while the fluid viscosity varies during the dispensing process. The information content of each system can determine which system is the best design for a specific application. It should be noted that the computer program is presented in appendices.

In the case study, the viscosity of the fluid being dispensed is assumed to have the initial value of 65.0 Pa.s, and will change by ± 50% of the initial value due to the instability of the system temperature in a dispensing process. The following function requirements are set and must be satisfied for the dispensing system:

FR_1 = steady-state flow rate of the fluid dispensed. It must be 20 mg/s with a tolerance of ± 1% of its value.

FR_2 = amount of the fluid dispensed. It must be 2 mg with a tolerance of ± 1% of its value.

The structural parameters, the operational parameters, and the fluid characterization used in the case study are presented in Table 6.1. To achieve the required flow rate and the amount of fluid dispensed, Equations (6.9) - (6.12) were used to calculate the required magnitude of the rotation speed ω and the duration of the control action T_d. The calculated results are listed in Table 6.2. If the fluid viscosity changes by ± 50%, the steady state flow rate and the amount of fluid dispensed were simulated by using the model developed in this chapter for Newtonian fluids. Equation (6.4) was then used to calculate the information content of the rotary-screw dispensing system for this specific situation, the results are given in Table 6.3, along with the calculated information contents of the time-pressure and positive-displacement dispensing systems in one of our previous studies [Chen et al. 2005]. It can be seen that the information content of the positive-displacement system is 1.337 bits, 6.572 for the rotary-screw dispensing system, and 12.119 bits for the time-pressure dispensing system. Based on this calculated information content, it can be concluded that if the fluid viscosity varies in a dispensing process, the positive-displacement system is the best design, followed by the rotary-screw dispensing system and the time-pressure dispensing system.

Table 6.1. Structural and operational parameters of the dispensing systems used in the case study.

Rotary-Screw Dispensing System	Parameters	Values
Structural parameters	Outer diameter of screw, D_{sw}	3.4 mm
	Channel depth, H	0.57 mm
	Cross channel width, W	3.3 mm
	Helix angle of the screw, φ	17 degrees
	Length in down channel direction, L_z	54 mm
	Fluid pressure at the top of syringe, P_s	1.0×10^5 +692 Pa
Operational parameters	Needle diameter, D_n	1.3 mm
	Needle length, L_n	18 mm
	Fluid pressure at the exit of needle, P_a	1.0×10^5 +692 Pa
	System temperature, T	25°C
Fluid properties	Density, ρ	950.2 kg/m^3
	Bulk modulus, B	1×10^9 Pa

Table 6.2. Magnitude and the duration of the control action.

Rotary-Screw Dispensing System	Parameters Values
Magnitude	16.90 rad/s
Duration	100 ms

Table 6.3. System ranges and information contents when the fluid viscosity changes by ±50%.

		Time- pressure	Rotary-Screw	Positive-Displacement
System range	**FR_1(mg/s)**	**13.333 ~ 40.0**	**18.304 ~ 22.042**	**20**
	FR_2 (mg)	**1.33 ~ 4.003**	**1.830 ~ 2.204**	**1.921 ~ 2.202**
Information content (IC) (bits)	**FR_1**	**6.059**	**3.286**	**0**
	FR_2	**6.060**	**3.286**	**1.337**
Total IC (bits)		**12.119**	**6.572**	**1.337**

6.5. Summary

This chapter presents the development of an integrated approach for the design of fluid dispensing systems based on the independence axiom and the information axiom. At first, the two fundamental principles of independence and information axioms were briefly reviewed and outlined. As the axiomatic design is processed in a conceptual or system level, a primitive or approximate model is sufficient to be used in the design process. For this purpose, the model developed in the preceding chapters was simplified in this chapter by assuming that the fluid being dispensed is Newtonian. Based on the simplified model, the development of an integrated approach for the design of fluid dispensing systems based on the independence axiom and the information axiom was then illustrated.

To show the effectiveness of the approach, a case study was carried out to evaluate the information content of the three different dispensing systems for the case where the fluid viscosity varies during the dispensing process. It has been shown that the positive-displacement system is the best design, followed by the rotary-screw dispensing system and the time-pressure dispensing system. It should be noted that this approach can be used not only to evaluate the existing dispensing systems, but also to design new dispensing systems.

7. CONCLUSIONS AND FUTURE WORK

7.1. Conclusions

Fluid dispensing is a complex process, which is in an interdisciplinary area involving electronic packaging, fluid mechanics, material science, control systems, and manufacturing. The present research is aimed to carry out a study on the modeling of the rotary-screw dispensing system. The main contributions of this research are summarized as follows:

1. For the characterization of the flow behavior, some empirical models such as the power law and the generalized power law equations were examined and the methods to determine the model parameters were discussed. In this study, the method of determining model parameter from a few dispensing experiments was used and by experiment this method was illustrated to be very promising and also cost-effective compared to the method of using a rheometer.

2. The flow in screw channels and circular tubes was examined and on this basis, a model to represent the steady state flow rate of fluid dispensed was presented for the rotary-screw dispensing system. By experiments, it was shown that this model is promising to predict the flow rate. Also, it was shown that the effects of the flow

behavior, the applied air pressure, the system temperature, and the needle diameter on the flow rate of fluid dispensed for given screw rotational speeds can be specified by using the model developed.

3. A model to represent the dynamics of the flow rate of fluid dispensed in the rotary-screw dispensing process was developed, by taking into account the fluid flow behavior, compressibility, and inertia. Based on the model developed, it was concluded that the dynamics of the flow rate of fluid dispensed to the rotation speed of the screw is equivalent to the second order system. Also by simulations, it was shown that the inconsistency of the amount of fluid dispensed can be investigated based on the model developed.

4. An approach was developed based on the axiomatic design, to integrate modeling into the design of dispensing systems. Based on the approach, the system performance of the rotary-screw dispensing system was evaluated and then compared to that of the time-pressure and positive-displacement dispensing systems. It is concluded that if the fluid viscosity varies in a dispensing process, the positive-displacement system is the best design, followed by the rotary-screw dispensing system and the time-pressure dispensing system.

7.2. Future Work

On the basis of the present study, future work is suggested as follows:

1. Experimentally verifying the dynamic model developed in this study. For this purpose, experiments of dispensing small amounts of fluid should be conducted and in each of the experiments, the amount of fluid dispensed should be measured by means of a micro-balance. The obtained experimental results would be compared with the simulation ones by using the dynamic model developed in this study.

2. Developing a new dynamic model by taking into account fluid compressibility and time-dependent fluid behavior simultaneously. It should be noted that in this study, the influence of time-dependent fluid behavior on the amount of fluid dispensed was not considered. Therefore, it would be interesting to examine how it affects the amount of fluid dispensed.

REFERENCES

[1] Babiarz, A. J., 1997, "Die Encapsulation and Flip Chip Underfilling Processes for Area Array Packaging of Advanced Integrated Circuits," *Asymtek Technical Report*.

[2] Babiarz, A. J., and Huysmans, F., 1997, "Reliability and Process Control in a Variety of Dispensing Applications," *Asymtek Technical Report*.

[3] Babiarz, A. J., Kiocke, D. La. J., and Lewis, A., 1970, "Engineering Principles of Plasticating Extrusion," *Proc. of Robert E. Krieger Publishing Company, Inc.*, Chapter 6, pp. 217.

[4] Barnes, H. A., Hutton, J. F., and Walters, K., 1989, "An Introduction to Rheology," *Elsevier Science Publishers B. V.*, pp. 1-37.

[5] Benezech, T., and Maingonnat, J.F., 1994, "Characterization of the Rheological Properties of Yogurt – A Review," *Journal of Food Engineering*, Vol. 21, pp. 4447-472.

[6] Bush, R., 1997, "Matching Fluid Dispensing to Materials for Electronics Applications," *Electronic Packaging & Production*, Vol. 37, pp. 56-62.

[7] Campbell, A. G., Sweeney, P. A., and Felton, J. N., 1992, "Experimental investigation of the drag flow assumption in extruder analysis," *Polymer Engineering and Science*, Vol. 32, pp. 1765-70.

[8] Chen, X. B., Schoenau, G., and Zhang, W. J., 1999, "Issues on Dispensing in Surface Mount Technology (SMT)," *Proc. International Conference on Advanced Manufacturing Technology*, China.

[9] Chen, X. B., Schoenau, G., and Zhang, W. J., 2001, "Dynamic Modeling of the Flow Rate in Time-Pressure Fluid Dispensing Processes," *The PACIFIC RIM/international, Intersociety, Electronic Packaging Technical/Business Conference & Exhibition*, Hawaii, USA.

[10] Chen, X. B., Schoenau, G., and Zhang, W. J., 2002, "On the Flow Rate Dynamics in Time-pressure Dispensing Processes," *ASME Journal of Dynamic Systems, Measurement, and Control*, Vol. 124, pp. 669-698.

[11] Chen, X. B., Pharaoh J. G., and Sugenor B. W., 2003, "Theoretical investigation into the performance of the Positive Displacement Dispensing Process," *Proc. of IMECE*, Vol. 03-42739, pp.16-21.

[12] Chen, X. B., and Kai, J., 2004, **"**Modeling of Positive-Displacement Fluid Dispensing Processes," *IEEE Transactions on Electronics Packaging Manufacturing*, Vol. 27, No. 3, pp. 157-163.

[13] Chen, X. B., and Ke, H., 2006, "Effects of Fluid Properties on Dispensing Processes for Electronics Packaging," *IEEE Transactions on Electronics Packaging Manufacturing*, Vol. 29, No. 2.

[13] Chen, X. B., Hashemi, M., and Kai, J., 2005, "Integrated Modeling and Design Approach for Fluid Dispensing Systems," *Proc. of Integrated Design and Process Technology*, Beijing, China.

[14] Chen, X. B., and Hashemi, M., 2006, "Investigation into the Performance of the Rotary Screw Fluid Dispensing Processes," *CSME Forum, May 21-24, Delta Lodge at Kananaskis*, Alberta, Canada.

[15] Chhabra R. P., and Richardson, J. F., 1999, "Non-Newtonian Flow in the Process Industries," *Butterworth-Heinemann*.

[16] Choo, K. P., Neelakantan, N. R., and Pittman, J. F. T., 1980, **"**Experimental Deep-channel Velocity Profiles and Operating Characteristics for a Single-screw Extruder," *Polymer Engineering and Science*, Vol. 20, pp. 349-56.

[17] Dixon, D., Kazalski, J., Murch, F., and Marongelli, S., 1997, "Practical Issues Concerning Dispensing Pump Technologies," *Circuits Assembly, August,* pp.36-40.

[18] Han, S., and Wang, K. K., 1997a, "Analysis of the Flow of Encapsulant During Underfill Encapsulation of Flip-Chips," *IEEE Trans. Components, Packaging, and Manufaturing Technology – Part B*, Vol. 20, pp. 424-433.

[19] Han, S., and Wang, K. K., 1997b, "Study on the Pressurized Underfill Encapsulation of Flip-Chips," *IEEE Trans. Components, Packaging, and Manufacturing Technology – Part B*, Vol. 20, pp. 434-442.

[20] Holdsworth, S. D., 1993, "Rheological Models Used for the Prediction of the Flow Properties of Food Products: a Literature Review," *Trans. Institution of Chemical Engineering*, Vol. 71(C3), pp. 139-179.

[21] Hong, Y. P., and Li, H. X., 2003, **"**Comparative Study of Fluid Dispensing Modeling," *IEEE Transactions on Electronics Packaging Manufacturing*, Vol. 26, No. 4, pp. 273-280.

[22] Irvine, T. F., and Capobianchi, M., 1998, "Non-Newtonian Flows, CRC Handbook of Mechanical," *Editor-in-Chief: Krieith F., CRC Press, Florida*, pp. 114-127, 1998.

[23] Krieger, M., and Behler, S., 1998, "Stability Aspects of Volumetric Epoxy Dispense," *Test & Assembly Seminarin*, Singapore.

[24] Laplace, P. S., 1806, "Mechanique Celeste," Supplement to Book 10.

[25] Li, Y., and Hsieh, F., 1994, "New Melt Conveying Models for a Single Screw Extruder," *Journal of Food Process Engineering*, Vol. 17, pp. 299-324.

[26] Li, Y., and Hsieh, F., 1996, "Modeling of Flow in a Single Screw Extruder," *Journal of Food Engineering*, Vol. 27, pp. 353-375.

[27] Li, H.-X., Tso, S. K., and Deng, H., 2001, "A Conceptual Approach to Integrate Design and Control for the Epoxy Dispensing Process," *Int. Adv. Manuf. Tchenol.*, Vol. 17, pp. 677-682.

[28] McCarthy, K. L., Kauten, R. J., and Agemura, C. K., 1992, **"**Application of NMR imaging to the study of velocity profiles during extrusion processing," *Trends in Food Science and Technology*, Vol. 3, pp. 215-19.

[29] Murch, F., Dixon, D., and Davis, M., 1997, "Issues for the Practical Production Use of Dispensing Technologies," *NEPCON WEST'97*, pp. 245-256.

[30] Ness, C. Q., and Lewis, A.R., 1997, "Best Practices in Surface Mount Adhesive Dispensing," *Asymetek Technical Report*.

[31] Nguyen, Q. D., and Boger, D. V., 1992, "Measuring the Flow Properties of Yield Stress Fluids," *Annu. Rev. Fluid Mech.*, Vol. 24, pp. 47-88.

[32] Quinones, H., Babiarz, A. J., and Adamson, S. J., 2000, "Flip Chip and Chip Scale Packaging Technologies: A Historical Perspective and Future Challenges," *SEMICON China 2000 Technical Symposium*.

[33] Rauwendaal, C., 1986, "Polymer Extrusion," *Hanser Publishers*, New York.

[34] Rauwendaal, C., 1989, **"**The ABC pf extruder screw design," *Advances in Polymer Technology*, Vol. 9, pp. 301-8.

[35] Rauwendaal, C. J., Osswald, T. A., Gramann, P. J., and Davis, B. A., 1999, **"**Design of Dispersive Mixing Sections," *Int. Polym. Proc.*, Vol. 13.

[36] Rauwendaal, C., 2004, "Polymer Extrusion," *Hanser Gardner Publication, Inc*.

[37] Razban, A., 1993, "Intelligent Control of an Automated Adhesive Dispensing Cell, Ph.D Thesis," *Imperial College*, London, UK.

[38] Razban, A., and Davies, B. L., 1995, "Analytical Modeling of the Automated Dispensing of Adhesive Material," *Journal of Adhesion Science Technology*, Vol. 9, pp. 1435-1450.

[39] Rowell, H. S., and Finalyson, D., 1922, **"**Screw viscosity pumps," *Engineering*, Vol. 114, pp. 606-7.

[40] Rowell, H. S., and Finlayson, D., 1928, "Screw viscosity pumps," *Engineering*, vol. 126, pp. 249-387.

[41] Skelland, A. H. P., 1967, "Non-Newtonian Flow and Heat Transfer," *John Wiley & Sons*, New York, pp.1-14.

[42] Suh, N. P., 2001, "Axiomatic Design: Advances and Applications," *Oxford University Press, Inc*.

[43] Tucker, C. L., 1989**,** "Fundamentals of Computer Modeling for Polymer Processing," *Hauser Publishers*, New York.

APPENDICES

[1] Computer program to verify the effectiveness of the steady state model developed in Chapter 3 with existing experiments.

% FILE NAME: Rotary_screw_static.m

% This program is used to investigate the performance of the rotary-screw dispensing process, which includes.

```
% 1. Identification of flow behavior index: n(dimensionless)in  power law equation and K0 and TK in(K=K0*exp(TK/T).
% 2. Verify the model by using the experiments results under the dispensing conditions which are different
%    from the parameter identification in (1).
% 3. Simulations to investigate various effects on the flow rate.


clc,clear,clf,
global Den H W Dsw angle Dn Ln Ls Lt Dt Omega FR_M;

%1. Experiment settings

Den = 1500.0;            % Density (kg/(m*m*m))
S_tension = 0.5;         % Fluid surface tension (N/m)

H = 0.57e-3;             % Channel depth (m)
W = 3.266e-3;            % Cross channel width (m)
Dsw = 3.4e-3;            % Outer diameter of the screw (m)
angle = 17*pi/180;       % Helix angle of the screw (rad)
Dn = 0.8382e-3;          % Needle internal diameter(m)
Ln = 25.4e-3;            % Length of Needle (m)
Ls = 16.0e-3;            % Length of Syringe (m)
Lt = 50.0e-3;            % Feed tube length (m)
Dt = 3.0e-3;             % Feed tube diameter (m)

Speed = 7.0;                % Screw speed (rps)
Omega = 2*pi*Speed;         % Screw speed (rad/s)


% 2. Estimate of [n K0 TK]

P = [1.0 2.0 3.0 4.0 3.0 3.0 3.0]'*1.0e+5 - S_tension/(Dn/2);      % Supplied pressure(Pa)
T = [60 60 60 60 40 60 80]';                                       % Needel temperature (oC)
FR_M = [37.60 39.68 43.14 46.41 36.62 43.14 50.42]';               % Measured flow rate (mg/s)
PT = [P T];
Err = [0 0 0 0 0 0 0]';
Paras = [0.8 60 40]';                                              % initial parameter estimates of [n K0 TK].
parashat = nlinfit(PT, Err, 'Relative_error_fun', Paras);

n = parashat(1)
K0 = parashat(2)
TK = parashat(3)


% 3. Model verification
P = [1.0 2.0 3.0 4.0]*1e+5;
```

```
FR_M = [33.26 34.76 36.62 39.31
        37.60 39.68 43.14 46.41
        41.36 44.42 50.42 54.66];          % Measured flow rate (mm^3/s)

P_simu = [0.5:0.01:4.5]*1.0e+5;

for j = 1:3
T = (j+1)*20;
K = K0*exp(TK/T);                          % Consistency Index (Pa.s^n)

md1 = pi*n*Dt^((3*n+1)/n)/(2^(3*n+2)*(3*n+1)*Lt^(1/n));
c1 = md1/(K^(1/n));
md3 = pi*n*Dn^((3*n+1)/n)/(2^(3*n+2)*(3*n+1)*Ln^(1/n));
c3 = md3/(K^(1/n));

md = power((Dsw*Omega*cos(angle)/(2*H)),(1-n));
md22 = md*W*H^3*sin(angle)/(4*(1+2*n)*Ls);
c22 = md22/K;
a = md22/md1^n + md22/md3^n;               % a is a scalar, not depending on T

c21 = (4+n)*W*H*Dsw*cos(angle)/20;
b = c21*Omega + c22.*(P_simu - S_tension/(Dn/2));

for i=1:length(P_simu)
%Find Qfrom the equation: Q + a * Q^n = b (Q has unit of m^3/s),
%or Q + a * a^n * 10^(9*(1-n)) = b*1.0e9 (Q has unit of mm^3/s)

Q = 10;                                    % Starting search with Q = 10 mm^3/s;
max_error = b(i)/1000;                     % Define the maximum error
step = b(i)/(1+a)/1000;                    % Define the step for calculating sensitivity
F = Q + a * Q^n*10^(9*(1-n))- b(i)*1.0e9;
while abs(F) > max_error
Q1 = Q-step;     F1 = Q1 +a * Q1^n*10^(9*(1-n)) - b(i)*1.0e9;
Q2 = Q+step;     F2 = Q2 +a * Q2^n*10^(9*(1-n)) - b(i)*1.0e9;
S = (F2-F1)/step/2;                        % Caculating the sensitivity

if S==0 F=0
elseif Q < 0
Q = step;                                  % Q must be a positive number
else
Q = Q - F/S;                               % Update Q based on F and S
F = Q + a * Q^n*10^(9*(1-n))-b(i)*1.0e9;
end
end
FR_simu(i) = Q*Den*1.0e-3;                 % Simulated flow rate (mg/s)
end

plot(P_simu*1.0e-3,FR_simu,'k-', P*1.0e-3,FR_M(j,:),'ko');
hold on;

end
legend('Model prediction','Measured Values',2)
axis ([50 450 20 70]);
grid;
xlabel('Presssure (KPa)');
ylabel('Flow Rate of Fluid Dispensed (mg/s)');
text (340,57, 'T = 80 ^oC');
text (340,47, 'T = 60 ^oC');
text (340,39, 'T = 40 ^oC');


% 4. Simulations

% 4.1 Q-Speed at different values of the power low index (n)
clear FR_simu;
pause;
clf;
P_simu = 2.0e+5;
Speed = [0.01:0.05:10.0];                  % Screw speed (rps)
Omega = 2*pi*Speed;                        % Screw speed (rad/s)
```

```
T = 60;                                          % Temperature (oC)
K = K0*exp(TK/T);                                % Consistency index (Pa.s^n)

for j=1:4
n = 1-(j-1)*0.15;

md1 = pi*n*Dt^((3*n+1)/n)/(2^(3*n+2)*(3*n+1)*Lt^(1/n));
c1 = md1/(K^(1/n));
md3 = pi*n*Dn^((3*n+1)/n)/(2^(3*n+2)*(3*n+1)*Ln^(1/n));
c3 = md3/(K^(1/n));

md = power((Dsw.*Omega*cos(angle)/(2*H)),(1-n));
md22 = md*W*H^3*sin(angle)/(4*(1+2*n)*Ls);
c22 = md22/K;
a = md22/md1^n + md22/md3^n;

c21 = (4+n)*W*H*Dsw*cos(angle)/20;
b = c21.*Omega +c22.*(P_simu - S_tension/(Dn/2));

for i=1:length(Speed)
%Find Qfrom the equation: Q + a * Q^n = b (Q has unit of m^3/s),
%or Q + a * a^n * 10^(9*(1-n)) = b*1.0e9 (Q has unit of mm^3/s)

Q = 10;                                          % Starting search with Q = 10 mm^3/s;
max_error = b(i)/1000;                           % Define the maximum error
step = b(i)/(1+a (i))/1000;                      % Define the step for calculating sensitivity
F = Q + a(i)* Q^n*10^(9*(1-n)) - b(i)*1.0e9;
while abs(F) > max_error
Q1 = Q-step;     F1 = Q1 +a(i) * Q1^n*10^(9*(1-n)) - b(i)*1.0e9;
Q2 = Q+step;     F2 = Q2 +a(i) * Q2^n*10^(9*(1-n)) - b(i)*1.0e9;
S = (F2-F1)/step/2;                              % Caculating the sensitivity

if S==0 F=0
elseif Q < 0
Q = step;                                        % Q must be a positive number
else
Q = Q - F/S;                                     % Update Q based on F and S
F = Q + a(i) * Q^n*10^(9*(1-n))-b(i)*1.0e9;
end
end
FR_simu(i) = Q*Den*1.0e-3;                       % Simulated flow rate (mg/s)
end

plot(Speed,FR_simu,'k-');
hold on;

end

grid;
title ('At Different Values of the Power Law Index');
xlabel('Screw Rotational Speed (rps)');
ylabel('Flow Rate of Fluid Dispensed (mg/s)');
text(7.5,273, 'n = 0.55');
text(7.5,140,'n = 0.70');
text(7.5,81, 'n = 0.85');
text(7.5,55, 'n = 1.00');

% 4.2 Q-Speed at differnt values of the applied air pressure (P)
clear FR_simu;
pause;
clf;

n = 0.7
Speed = [0.01:0.05:10.0];                        % Screw speed (rps)
Omega = 2*pi*Speed;                              % Screw speed (rad/s)
T = 60;                                          % Temperature (oC)
K = K0*exp(TK/T);                                % consistency Index (Pa.s^n)
for j=1:4
P_simu = j*1.0e+5;
```

```
md1 = pi*n*Dt^((3*n+1)/n)/(2^(3*n+2)*(3*n+1)*Lt^(1/n));
c1 = md1/(K^(1/n));
md3 = pi*n*Dn^((3*n+1)/n)/(2^(3*n+2)*(3*n+1)*Ln^(1/n));
c3 = md3/(K^(1/n));

md = power((Dsw.*Omega*cos(angle)/(2*H)),(1-n));
md22 = md*W*H^3*sin(angle)/(4*(1+2*n)*Ls);
c22 = md22/K;
a = md22/md1^n + md22/md3^n;

c21 = (4+n)*W*H*Dsw*cos(angle)/20;
b = c21.*Omega + c22.*(P_simu - S_tension/(Dn/2));

for i=1:length(Speed)
%Find Qfrom the equation: Q + a * Q^n = b (Q has unit of m^3/s),
%or Q + a * a^n * 10^(9*(1-n)) = b*1.0e9 (Q has unit of mm^3/s)

Q = 10;                                                    % Starting search with Q = 10 mm^3/s;
max_error = b(i)/1000;                                     % Define the maximum error
step = b(i)/(1+a (i))/1000;                                % Define the step for calculating sensitivity
F = Q + a(i)* Q^n*10^(9*(1-n)) - b(i)*1.0e9;
while abs(F) > max_error
Q1 = Q-step;     F1 = Q1 + a(i) * Q1^n*10^(9*(1-n)) - b(i)*1.0e9;
Q2 = Q+step;     F2 = Q2 + a(i) * Q2^n*10^(9*(1-n)) - b(i)*1.0e9;
S = (F2-F1)/step/2;                                        % Caculating the sensitivity

if S==0 F=0
elseif Q < 0
Q = step;                                                  % Q must be a positive number
else
Q = Q - F/S;                                               % Update Q based on F and S
F = Q + a(i) * Q^n*10^(9*(1-n))-b(i)*1.0e9;
end
end
FR_simu(i) = Q*Den*1.0e-3;                                 % Simulated flow rate (mg/s)
end

plot(Speed,FR_simu,'k-');
hold on;

end

grid;
title ('At Different Values of the Applied Air Pressure');
xlabel('Screw Rotational Speed (rps)');
ylabel('Flow Rate of Fluid Dispensed (mg/s)');
text(7.5,210, 'Pp = 4 Bar');
text(7.5,175, 'Pp = 3 Bar');
text(7.5,140, 'Pp = 2 Bar');
text(7.5,110, 'Pp = 1 Bar');

% 4.3 Q-Speed at differnt values of temperature (T)
clear FR_simu;
pause;
clf;

n = 0.7
speed = [0.01:0.05:10.0];                  % Screw speed (rps)
Omega = 2*pi*Speed;                        % Screw speed (rad/s)
P_simu = 2.0e+5;

for j=1:4

T = (j+1)*20;                              % Temperature (oC)
K = K0*exp(TK/T);                          % consistency Index (Pa.s^n)

md1 = pi*n*Dt^((3*n+1)/n)/(2^(3*n+2)*(3*n+1)*Lt^(1/n));
c1 = md1/(K^(1/n));
md3 = pi*n*Dn^((3*n+1)/n)/(2^(3*n+2)*(3*n+1)*Ln^(1/n));
c3 = md3/(K^(1/n));
```

```
md = power((Dsw.*Omega*cos(angle)/(2*H)),(1-n));
md22 = md*W*H^3*sin(angle)/(4*(1+2*n)*Ls);
c22 = md22/K;
a = md22/md1^n + md22/md3^n;

c21 = (4+n)*W*H*Dsw*cos(angle)/20;
b = c21.*Omega + c22.*(P_simu - S_tension/(Dn/2));

for i=1:length(Speed)
%Find Q from the equation: Q + a * Q^n = b (Q has unit of m^3/s),
%or Q + a * a^n * 10^(9*(1-n)) = b*1.0e9 (Q has unit of mm^3/s)

Q = 10;                                          % Starting search with Q = 10 mm^3/s;
max_error = b(i)/1000;                           % Define the maximum error
step = b(i)/(1+a (i))/1000;                      % Define the step for calculating sensitivity
F = Q + a(i)* Q^n*10^(9*(1-n)) - b(i)*1.0e9;
while abs(F) > max_error
Q1 = Q-step;     F1 = Q1 + a(i) * Q1^n*10^(9*(1-n)) - b(i)*1.0e9;
Q2 = Q+step;     F2 = Q2 + a(i) * Q2^n*10^(9*(1-n)) - b(i)*1.0e9;
S = (F2-F1)/step/2;                              % Caculating the sensitivity

if S==0 F=0
elseif Q < 0
Q = step;                                        % Q must be a positive number
else
Q = Q - F/S;                                     % Update Q based on F and S
F = Q + a(i) * Q^n*10^(9*(1-n))-b(i)*1.0e9;
end
end
FR_simu(i) = Q*Den*1.0e-3;                       % Simulated flow rate (mg/s)
end

plot(Speed,FR_simu,'k-');
hold on;

 end

grid;
title ('At Different Values of temperature');
xlabel('Screw Rotational Speed (rps)');
ylabel('Flow Rate of Fluid Dispensed (mg/s)');
text(7.5,257, 'T = 100 ^oC');
text(7.5,198, 'T = 80 ^oC');
text(7.5,143, 'T = 60 ^oC');
text(7.5,95,  'T = 40 ^oC');

% 4.4 Q-Speed at differnt values of the needle diameter (Dn)
clear FR_simu;
pause;
clf;

n = 0.7
Speed = [0.01:0.05:10.0];                        % Screw Speed (rps)
Omega = 2*pi*Speed;                              % Screw Speed (rad/s)
T = 60;                                          % Temperature (oC)
K = K0*exp(TK/T);                                % consistency Index (Pa.s^n)
P_simu = 2.0e+5;

Needle_diameter = [0.41 0.58 0.84 1.60]*1.0e-3;
for j=1:4
Dn = Needle_diameter (j);

md1 = pi*n*Dt^((3*n+1)/n)/(2^(3*n+2)*(3*n+1)*Lt^(1/n));
c1 = md1/(K^(1/n));
md3 = pi*n*Dn^((3*n+1)/n)/(2^(3*n+2)*(3*n+1)*Ln^(1/n));
c3 = md3/(K^(1/n));

md = power((Dsw.*Omega*cos(angle)/(2*H)),(1-n));
md22 = md*W*H^3*sin(angle)/(4*(1+2*n)*Ls);
c22 = md22/K;
```

```
a = md22/md1^n + md22/md3^n;

c21 = (4+n)*W*H*Dsw*cos(angle)/20;
b = c21.*Omega + c22.*(P_simu - S_tension/(Dn/2));

for i=1:length(Speed)
%Find Q from the equation: Q + a * Q^n = b (Q has unit of m^3/s),
%or Q + a * a^n * 10^(9*(1-n)) = b*1.0e9 (Q has unit of mm^3/s)

Q = 10;                                          % Starting search with Q = 10 mm^3/s;
max_error = b(i)/1000;                           % Define the maximum error
step = b(i)/(1+a (i))/1000;                      % Define the step for calculating sensitivity
F = Q + a(i)* Q^n*10^(9*(1-n)) - b(i)*1.0e9;
while abs(F) > max_error
Q1 = Q-step;     F1 = Q1 + a(i) * Q1^n*10^(9*(1-n)) - b(i)*1.0e9;
Q2 = Q+step;     F2 = Q2 + a(i) * Q2^n*10^(9*(1-n)) - b(i)*1.0e9;
S = (F2-F1)/step/2;                              % Caculating the sensitivity

if S==0 F=0
elseif Q < 0
Q = step;                                        % Q must be a positive number
else
Q = Q - F/S;                                     % Update Q based on F and S
F = Q + a(i) * Q^n*10^(9*(1-n))-b(i)*1.0e9;
end
end
FR_simu(i) = Q*Den*1.0e-3;                       % Simulated flow rate (mg/s)
end

plot(Speed,FR_simu,'k-');
hold on;

end

grid;
title ('At Different Values of the Needle Diameter');
xlabel('Screw Rotational Speed (rps)');
ylabel('Flow Rate of Fluid Dispensed (mg/s)');
text(7,205, 'Dn = 1.60 mm');
text(7,140, 'Dn = 0.84 mm');
text(7,72, 'Dn = 0.58 mm');
text(7,28, 'Dn = 0.41 mm');

 % The End
```

function Error = Relative_error_fun(Paras, x)

```
% This function gives the relative error, i.e.,
% Error = (Q + a*Q^n - b)/Q
% where Q is the measured flow rate


global Den H W Dsw angle Dn Ln Ls Lt Dt Omega FR_M;

n = Paras(1);
K0 = Paras(2);
TK = Paras(3);
P = x(:,1);
T = x(:,2);

K = K0*exp(TK./T);                               % Consistency Index (Pa.s^n)

md1 = pi*n*Dt^((3*n+1)/n)/(2^(3*n+2)*(3*n+1)*Lt^(1/n));
c1 = md1/(K.^(1/n));
md3 = pi*n*Dn^((3*n+1)/n)/(2^(3*n+2)*(3*n+1)*Ln^(1/n));
c3 = md3/(K.^(1/n));

md = power((Dsw*Omega*cos(angle)/(2*H)),(1-n));
md22 = md*W*H^3*sin(angle)/(4*(1+2*n)*Ls);
```

```
c22 = md22./K;
a = md22/md1^n + md22/md3^n;                    % a is a scalar, not depending on T

c21 = (4+n)*W*H*Dsw*cos(angle)/20;
b = c21*Omega + c22.*P;

FR_M_V = FR_M*1.0e-6/Den;                       % Measured flow rate (m^3/s)
Error = (FR_M_V + a*FR_M_V.^n - b)./FR_M_V      % Rlative error

% The End of Function
```

[2] Computer program to investigate the performance of the rotary-screw dispensing system using the dynamic model developed in chapter 4.

% This program is used to investigate the performance of the rotary-screw dispensing system for non-Newtonian Flow.

```
clc, clear, clf,

% 1. Parameters for Simulation


g = 9.8;                        % Gravity accelaration
Dens = 1500;                    % Density of the Fluid (Kg/m^3)
T = 30;                         % Needle Temperature, (degree)
n = 0.994;                      % Fluid  behavior Index
T_0 = 0;                        % Yield stress as a function of temperature
K =1.446*exp(146.23/T);         % Consistency index
B = 1e9;                        % Bulk modulus of fluid (pa)
Dn = 0.8382e-3;                 % Intermal diameter of the needle (m)
An = pi*Dn^2/4;                 % Needle cross section area (m^2)
Ln = 25.4e-3;                   % Length of the needle (m)
H = 0.57e-3;                    % Channel depth (m)
W = 3.266e-3;                   % Cross channel width (m)
Dsw = 3.40e-3;                  % Outer diameters of the screw (m)
Dr= 2.26e-3;                    % Root diameter (m)
ph = 17*pi/180;                 % Helix angle of the screw (rad)
Ls = 16.0e-3;                   % Lenght of the syringe (m)
Lz = Ls/sin(ph);                % Lenght of the down channel in z direction (m)
Vs = pi*(Dsw^2-Dr^2)*Ls/4;      % Volume of the fluid in the syringe (m^3)
Speed = 7.0;                    % Screw speed (rps)
w = 2*pi*Speed;                 % Screw speed (rad/s)
Vbz = (Dsw*cos(ph)*w)/2;        % velocity along z direction (m/s)
Visc = K*((Vbz/H)^(n-1));       % viscosity of fluid for non-Newtonian flow behavior (pa.s)
Cw = (4+n)*W*H*Dsw*cos(ph)/20;      % Coefficient associated with the pure drag flow (m^3)
Cp = (W*H^3)/(4*(1+2*n)*Visc*Lz);   % Coefficient associated with the pure pressure flow (m^3/pa.s)


Case_study =  'case_4';                         % For simulation, input and change the "case_n" here
switch Case_study

% 2. Influence of dispensing time (with ODE23tb Max. step size 0.001)

case {'case_1'}                                 % Response of the flow rate with different T_p
T_vector = [0.001 0.003 0.010 0.045];           % Vector of the time period of the screw rotation (s)

for i=1:4
T_p = T_vector(i);
T_final = 0.10;                                 % Simulation time
[t,x,y] = sim('rotary_screw_fdmodelnn', T_final);
flow_rate = y(:,1)*Dens*1e6;                    % Volume of fluid extruded from the needle, mg/s
plot(t, flow_rate,'k-');
```

```
hold on;
end

axis ([0 0.10 0 40]);
grid;
xlabel('t (s)'); ylabel('Flow Rate (mg/s)');
pause;
clf;

T_p = 0.045;
T_final = 0.10;                                          % Simulation time (s)
[t,x,y] = sim('rotary_screw_fdmodelnn', T_final);
Qu = max (y(:,1))/max (y(:,3))

i = 1;
for T_p = 0.001:0.001:0.045
T_final = 0.10;                % Simulation time (s)
[t,x,y] = sim('rotary_screw_fdmodelnn', T_final);
T_p
amount = y(end,2)*Dens*1e6                               % Volume of fluid extruded from the needle (mg/s)
Qs = (w*Cw*T_p*Dens*1e6)/(1+Cp/Qu)
err = 100*(amount-Qs)/Qs;
if i==1
err_v = err;
Qs_v = Qs;
else
err_v = [err_v err];
Qs_v = [Qs_v Qs];
end
i=i+1;
end
plot(Qs_v, err_v,'k-');
grid;
xlabel('Design Amount (mg)'); ylabel('Error (%)');

% 3. Influence of needle temprature (with ODE23tb Max. step size 0.0001)

case {'case_2'}                                          % Influence of the temperature
T_p = 0.002;                                             % Time dispensed (s)
T_vector = [27 35 45];                                   % Needel Temperature (degree)
for i=1:3
T = T_vector(i);
K =1.446*exp(146.23/T);                                  % Consistency index
Visc = K*((Vbz/H)^(n-1));
Cp = (W*H^3)/(4*(1+2*n)*Visc*Lz);
T_final = 0.10;              % Simulation time (s)
[t,x,y] = sim('rotary_screw_fdmodelnn', T_final);
flow_rate = y(:,1)*Dens*1e6;                             % Volume of the fluid dispensed from the needle (mg/s)
plot(t, flow_rate,'k-');
hold on;
end

axis ([0 0.02 0 50]);
grid;
xlabel('Time (s)'); ylabel('Flow Rate (mg/s)');
pause;
clf;

T=27 ;                                                   % Needel Temperature (degree)
K =1.446*exp(146.23/T);                                  % Consistency index
Visc = K*((Vbz/H)^(n-1));
Cp = (W*H^3)/(4*(1+2*n)*Visc*Lz);

T_p = 0.045;
T_final = 0.10;                                          % Simulation time (s)
[t,x,y] = sim('rotary_screw_fdmodelnn', T_final);
Qu = max (y(:,1))/max (y(:,3))

i = 1;
for T_p = 0.005:0.001:0.045
```

```
T_final = 0.10;                                  % Simulation time (s)
[t,x,y] = sim('rotary_screw_fdmodelnn', T_final);
T_p
amount = y(end,2)*Dens*1e6                       % Volume of the fluid dispensed from the needle (mg/s)
Qs= (w*Cw*T_p*Dens*1e6)/(1+Cp/Qu)
err= 100*(amount-Qs)/Qs
if i==1
err_v = err;
Qs_v = Qs;
else
err_v = [err_v err];
Qs_v = [Qs_v Qs];
end
i=i+1;
end
plot(Qs_v, err_v,'k-');
hold on;

T=35 ;                                           % Needel Temperature (degree)
K =1.446*exp(146.23/T);                          % Consistency index
Visc = K*((Vbz/H)^(n-1));
Cp = (W*H^3)/(4*(1+2*n)*Visc*Lz);

T_p = 0.045;
T_final = 0.10;                                  % Simulation time (s)
[t,x,y] = sim('rotary_screw_fdmodelnn', T_final);
Qu = max (y(:,1))/max (y(:,3))

i = 1;
for T_p = 0.005:0.001:0.045
T_final = 0.10;                                  % Simulation time (s)
[t,x,y] = sim('rotary_screw_fdmodelnn', T_final);
T_p
amount = y(end,2)*Dens*1e6                       % Volume of the fluid dispensed from the needle (mg/s)
Qs = (w*Cw*T_p*Dens*1e6)/(1+Cp/Qu)
err = 100*(amount-Qs)/Qs;
if i==1
err_v = err;
Qs_v = Qs;
else
err_v = [err_v err];
Qs_v = [Qs_v Qs];
end
i=i+1;
end
plot(Qs_v, err_v,'k-');
hold on;

T=45;                                            % Needel Temperature (degree)
K =1.446*exp(146.23/T);                          % Consistency index
Visc = K*((Vbz/H)^(n-1));
Cp = (W*H^3)/(4*(1+2*n)*Visc*Lz);

T_p = 0.045;
T_final = 0.10;                                  % Simulation time (s)
[t,x,y] = sim('rotary_screw_fdmodelnn', T_final);
Qu = max (y(:,1))/max (y(:,3))

i = 1;
for T_p = 0.005:0.001:0.045
T_final = 0.10;                                  % Simulation time (s)
[t,x,y] = sim('rotary_screw_fdmodelnn', T_final);
T_p
amount = y(end,2)*D  ens*1e6                     % Volume of the fluid dispensed from the needle (mg/s)
Qs = (w*Cw*T_p*Dens*1e6)/(1+Cp/Qu)
err = 100*(amount-Qs)/Qs
if i==1
err_v = err;
Qs_v = Qs;
else
```

```
err_v = [err_v err];
Qs_v = [Qs_v Qs];
end
i=i+1;
end
plot(Qs_v, err_v,'k-');
grid;
xlabel('Design Amount (mg)'); ylabel('Error (%)');


% 4. Influence of fluid compressibility (with ODE23tb Max. step size 0.0001)

case {'case_3'}
T_p = 0.002;                                    %time period of piston movement (s)

B_vector = [0.8e9 1e9 5e9];                     % Bulk modulus of the fluid in the syringe
for i=1:3
B = B_vector(i);
T_final = 0.10;                                 % Simulation time (s)
[t,x,y] = sim('rotary_screw_fdmodelnn', T_final);
flow_rate = y(:,1)*Dens*1e6;                    % Volume of the fluid dispensed from the needle (mg/s)
plot(t, flow_rate,'k-');
hold on;
end

axis ([0 0.02 0 50]);
grid;
xlabel('Time (s)'); ylabel('Flow Rate (mg/s)');
pause;
clf;

B=0.8e9;                                        %Bulk modulus of the fluid (pa)

T_p = 0.045;
T_final = 0.10;                                 % Simulation time (s)
[t,x,y] = sim('rotary_screw_fdmodelnn', T_final);
Qu = max (y(:,1))/max (y(:,3))

i = 1;
for T_p = 0.005:0.001:0.045
T_final = 0.10;                                 % Simulation time (s)
[t,x,y] = sim('rotary_screw_fdmodelnn', T_final);
T_p
amount = y(end,2)*Dens *1e6                     % Volume of the fluid dispensed from the needle (mg)
Qs = (w*Cw*T_p*Dens*1e6)/(1+Cp/Qu)
err = 100*(amount-Qs)/Qs;
if i==1
err_v = err;
Qs_v = Qs;
else
err_v = [err_v err];
Qs_v = [Qs_v Qs];
end
i=i+1;
end
plot(Qs_v, err_v,'k-');
hold on;

B=1e9;                                          %Bulk modulus of the fluid (pa)

T_p = 0.045;
T_final = 0.10;                                 % Simulation time (s)
[t,x,y] = sim('rotary_screw_fdmodelnn', T_final);
Qu = max (y(:,1))/max (y(:,3))

i = 1;
for T_p = 0.005:0.001:0.045
T_final = 0.10;                                 % Simulation time (s)
[t,x,y] = sim('rotary_screw_fdmodelnn', T_final);
T_p
```

```
amount = y(end,2)*Dens*1e6                          % Volume of the fluid dispensed from the needle (mg)
Qs = (w*Cw*T_p*Dens*1e6)/(1+Cp/Qu)
err = 100*(amount-Qs)/Qs;
if i==1
err_v = err;
Qs_v = Qs;
else
err_v = [err_v err];
Qs_v = [Qs_v Qs];
end
i=i+1;
end
plot(Qs_v, err_v,'k-');
hold on;

B=5e9;                                              %Bulk modulus of the fluid (pa)

T_p = 0.045;
T_final = 0.10;              % Simulation time (s)
[t,x,y] = sim('rotary_screw_fdmodelnn', T_final);
Qu = max (y(:,1))/max (y(:,3))

i = 1;
for T_p = 0.005:0.001:0.045
T_final = 0.10;                    % Simulation time (s)
[t,x,y] = sim('rotary_screw_fdmodelnn', T_final);
T_p
amount = y(end,2)*Dens*1e6                          % Volume of the fluid dispensed from the needle (mg)
Qs = (w*Cw*T_p*Dens*1e6)/(1+Cp/Qu)
err = 100*(amount-Qs)/Qs;
if i==1
err_v = err;
Qs_v = Qs;
else
err_v = [err_v err];
Qs_v = [Qs_v Qs];
end
i=i+1;
end
plot(Qs_v, err_v,'k-');
grid;
xlabel('Design Amount (mg)'); ylabel('Error (%)');


% 5. Influence of fluid behavior (with ODE23tb Max. step size 0.0001)

case {'case_4'}

T_p = 0.002;                                        % Time dispensed (s)
T = 25
K =1.446*exp(146.23/T)
n_vector = [0.7 0.9 0.99];                          % Fluid behavior Index
for i=1:3
n = n_vector(i);
Visc = K*((Vbz/H)^(n-1));
Cw = (4+n)*W*H*Dsw*cos(ph)/20;
Cp = (W*H^3)/(4*(1+2*n)*Visc*Lz);

T_final = 0.10;                                     % Simulation time (s)
[t,x,y] = sim('rotary_screw_fdmodelnn', T_final);
flow_rate = y(:,1)*Dens*1e6;   % Volume of the fluid dispensed from the needle (mg/s)
plot(t, flow_rate,'k-');
hold on;
end

axis ([0 0.02 0 50]);
grid;
xlabel('Time (s)'); ylabel('Flow Rate (mg/s)');
pause;
clf;
```

```
n=0.7;                                          % Fluid behavior Index
Visc = K*((Vbz/H)^(n-1));
Cw = (4+n)*W*H*Dsw*cos(ph)/20;
Cp = (W*H^3)/(4*(1+2*n)*Visc*Lz);

T_p = 0.045;
T_final = 0.10;                                 % Simulation time (s)
[t,x,y] = sim('rotary_screw_fdmodelnn', T_final);
Qu = max (y(:,1))/max (y(:,3))

i = 1;
for T_p = 0.0005:0.001:0.02
T_final = 0.10;                                 % Simulation time (s)
[t,x,y] = sim('rotary_screw_fdmodelnn', T_final);
T_p
amount = y(end,2)*Dens*1e6                      % Volume of the fluid dispensed from the needle (mg/s)
Qs= (w*Cw*T_p*Dens*1e6)/(1+Cp/Qu)
err= 100*(amount-Qs)/Qs;
if i==1
err_v = err;
Qs_v = Qs;
else
err_v = [err_v err];
Qs_v = [Qs_v Qs];
end
i=i+1;
end
plot(Qs_v, err_v,'k-');
hold on;

n=0.9 ;                                         % Fluid behavior Index
Visc = K*((Vbz/H)^(n-1));
Cw = (4+n)*W*H*Dsw*cos(ph)/20;
Cp = (W*H^3)/(4*(1+2*n)*Visc*Lz);

T_p = 0.045;
T_final = 0.10;                                 % Simulation time (s)
[t,x,y] = sim('rotary_screw_fdmodelnn', T_final);
Qu = max (y(:,1))/max (y(:,3))

i = 1;
for T_p = 0.0005:0.001:0.02
T_final = 0.10;                                 % Simulation time (s)
[t,x,y] = sim('rotary_screw_fdmodelnn', T_final);
T_p
amount = y(end,2)*Dens*1e6                      % Volume of the fluid dispensed from the needle (mg/s)
Qs = (w*Cw*T_p*Dens*1e6)/(1+Cp/Qu)
err = 100*(amount-Qs)/Qs;
if i==1
err_v = err;
Qs_v = Qs
else
err_v = [err_v err];
Qs_v = [Qs_v Qs];
end
i=i+1;
end
plot(Qs_v, err_v,'k-');
hold on;

n=0.99;                                         % Fluid behavior Index
Visc = K*((Vbz/H)^(n-1));
Cw = (4+n)*W*H*Dsw*cos(ph)/20;
Cp = (W*H^3)/(4*(1+2*n)*Visc*Lz);

T_p = 0.045;
T_final = 0.10;                                 % Simulation time (s)
[t,x,y] = sim('rotary_screw_fdmodelnn', T_final);
Qu = max (y(:,1))/max (y(:,3))
```

```
i = 1;
for T_p = 0.0005:0.001:0.02
T_final = 0.10;                                   % Simulation time (s)
[t,x,y] = sim('rotary_screw_fdmodelnn', T_final);
T_p
amount = y(end,2)*Dens*1e6                        % Volume of the fluid dispensed from the needle (mg/s)
Qs = (w*Cw*T_p*Dens*1e6)/(1+Cp/Qu)
err = 100*(amount-Qs)/Qs;
if i==1
err_v = err;
Qs_v = Qs
else
err_v = [err_v err];
Qs_v = [Qs_v Qs];
end
i=i+1;
end
plot(Qs_v, err_v,'k-');
grid;
xlabel('Design Amount (mg)'); ylabel('Error (%)');

end
%Then End
```

[3] Computer program to investigate the effectiveness of the integrated modeling and design approach developed in chapter 6.

```
% filename: information_content.m

% This program is used to elvaute the information content of Rotary-Screw dispensing for given flow rate and given amount.

clc, clear,
Q_given = 20                                      % Give the desired flow rate (mg/s)
A_given = 2                                       % Give the desired amount (mg)

% 1. Parameters for Simulation

T = 273+25;                                       % Average temperature in the system (K)
Dens = 950.2;                                     % Density of the Fluid (Kg/m^3)
Visc = 63.8;                                      % Initial viscosity of the Fluid (Kg/(m*s) or Pa*s)
B = 1e9;                                          % Bulk modulus of fluid (pa)
Dn = 1.3e-3;                                      % Intermal diameter of the needle (m)
Ln = 0.018;                                       % Length of the needle (m)
H = 0.57e-3;                                      % Channel depth (m)
W = 3.3e-3;                                       % Cross channel width (m)
Dsw = 3.4e-3;                                     % Outer diameters of the screw (m)
Dr = 2.26e-3;                                     % Root diameter (m)
ph = 17*pi/180;                                   % Helix angle of the screw (rad)
Ls = 16.0e-3;                                     % Lenght of the syringe (m)
Lz = Ls/sin(ph);                                  % Lenght of the down channel in z direction (m)
Vs = pi*(Dsw^2-Dr^2)*Ls/4;                        % Volume of the fluid in the syringe (m^3)
Cw = W*H*Dsw*cos(ph)/4;                           % Coefficient associated with the pure drag flow (m^3)
Cp = (W*H^3)/(12*63.8*Lz);                        % Coefficient associated with the pure pressure flow (m^3/pa.s)

% 2. Find the rotational speed and the dispensing time

% 2.1 Find the rotational speed required for the given mass flow rate
Qn = pi*power(Dn,4)/(128*Visc*Ln);                % Steady-state flow rate in the needle under unit pressure drop (m^3/Pa.s)
Qs = Cw/(1+Cp/Qn);                                % Steady-state flow rate under unit rotational speed (m^3/s/rad/s)
Ms = Qs*Dens*1.0e6;                               % Steady-state mass rate under unit rotational speed (mg/s/rad/s)
w = Q_given/Ms;                                   % Rotational speed needed for the given flow rate (Rad/s)
```

```
% 2.2 Find the dispensing time required for the given amount

w_width = 10;                                   % Initial dispensing time (ms)
Inc_width = 1;
a = Vs/(2*B*Qn);
b = 1+Cp/Qn;

while Inc_width > 0
% Evaluate the sensitivity of the amount to 0.1 ms
t_dispense = w_width/10;                        % % of period
[t,x,y] = sim('Rotary_Screw_fmodel',0.6);       % 0.6 is the simulation time, which is not equal to dispensing time
A1 = y(end,1);                                  % the amount of fluid dispensed

t_dispense = (w_width+1)/10;
[t,x,y] = sim('Rotary_Screw_fmodel',0.6);
A2 = y(end,1);
S = (A2-A1);                                    % Sensitivity of the amount to dispensing time, mg/ms

% Update the dispensing time
Inc_width = round((A_given - A1)/S);            % Increment of dispensing time (ms)
w_width = w_width +  Inc_width;
end
t_dispense =(w_width/10);
w_width= t_dispense*0.6/100;                    % Display the dispensing time (ms)

% 3. Evaluate the information content (IC) if the viscosity changes by +/- 50%

Visc_change = Visc*1.50;
Qn = pi*power(Dn,4)/(128*Visc_change*Ln);
Q1 = w*Dens*1e6*(Cw/(1+Cp/Qn));
a = Vs/(2*B*Qn);
b = 1+Cp/Qn;
[t,x,y] = sim('Rotary_Screw_fmodel',0.6);
A1 = y(end,1);

Visc_change = Visc*0.50;
Qn = pi*power(Dn,4)/(128*Visc_change*Ln);
Q2 = w*Dens*1e6*(Cw/(1+Cp/Qn));
a = Vs/(2*B*Qn);
b = 1+Cp/Qn;
[t,x,y] = sim('Rotary_Screw_fmodel',0.6);
A2 = y(end,1);

%Caculation of Information content
dr =0.02*20                                     % here suppose design range is +/- 0.01 of its value for s.s. flow rate and flow amount
if (Q2-Q1)< dr
IC_Q = 0                                        % Information content of flow rate
else
IC_Q =-log2(dr/(Q2-Q1))
end
dr =0.02*2                                      % here suppose design range is +/- 0.01 of its value for flow amount
if (A2-A1)< dr
IC_A = 0
else
IC_A =-log2(dr/(A2-A1))                         % Information content of flow amount

w_width

w
end
```